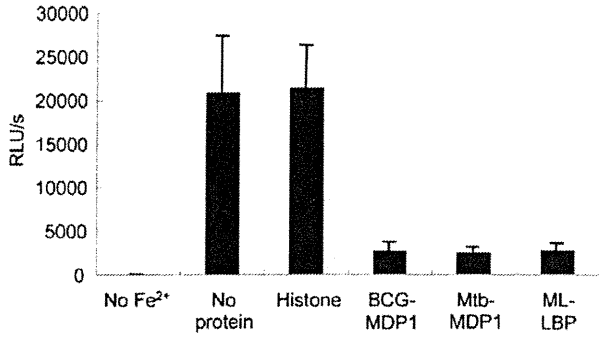

Figure 5. Mtb-MDP1 and ML-LBP suppress the generation of the hydroxyl radical by the Fenton reaction. The level of hydroxyl radical produced by the Fenton reaction was monitored using L-012, a probe that is sensitive to reactive oxygen, in the presence or absence of 3 μM proteins, such as bovine histone H1 (Histone), BCG-MDP1, Mtb-MDP1, and ML-LBP. The level of hydroxyl radical 10 sec after initiation of the reaction is shown. The data is representative of 3 independent experiments.
doi:10.1371/journal.pone.0020985.g005

slower but comparable with that of apo-horse ferritin (K_m value, 0.2127 mM) as shown in Figure S3. Taken together, to our knowledge, this is the first report of a molecule possessing iron oxidation and storage other than ferritin superfamily proteins.

The amino acid sequence of MDP1/ML-LBP resembles histones in eukaryotes and histone-like proteins in bacteria, thus it probably has a similar molecular root with those proteins. It is intriguing how MDP1/ML-LBP has evolved to acquire similar activity as ferritin superfamily proteins during evolution.

Mycobacteria are successful pathogens, producing various kinds of effector molecules that facilitate the long-term survival in the host. Acquisition of iron and preventing iron-dependent generation of ROS are essential events for the replication and survival in the host for the pathogens [9,34,35]. Dps is involved in the survival of bacterial pathogens, such as *Listeria* and *Salmonella*, by detoxifying iron [36]. Here we showed that Ms-MDP1 plays a critical role in iron detoxication in *M. smegmatis*, which produces Dps (Fig. 7). Therefore, it is reasonable to consider that MDP1/ML-LBP has more significant roles in the live and virulence of pathogenic mycobacteria, which lack Dps. That may be one of reasons why MDP1 is essential in *M. tuberculosis* [27]. Recent study conducted by Kumar et al, showing protection of DNA by MDP1

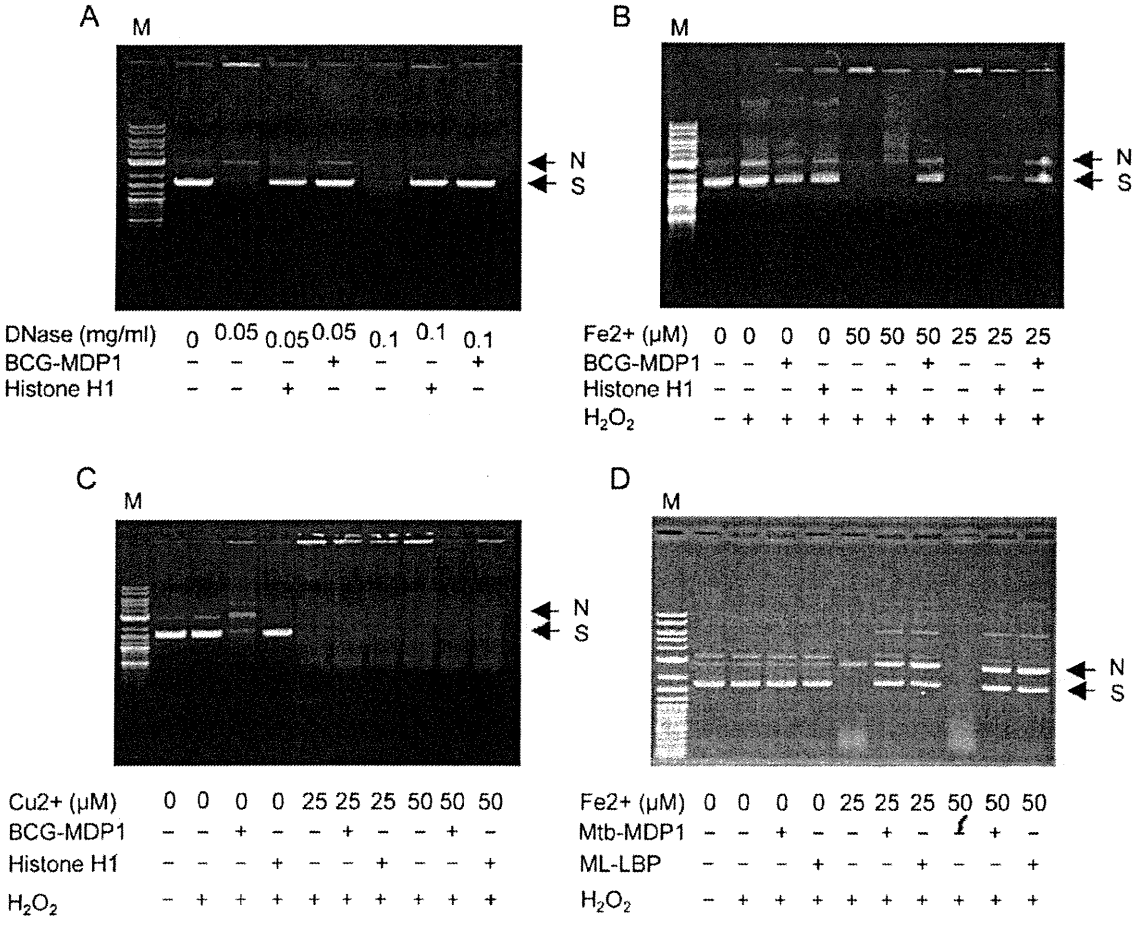

Figure 6. DNA protective activity of MDP1/ML-LBP. The plasmid DNA (pUC19) was treated with DNase 1 (A), H_2O_2 and $FeSO_4$ (Fenton reaction, B and C), and H_2O_2 and $CuSO_4$ (Fenton-like reaction, D) in the presence or absence of proteins, such as histone H1, BCG- MDP1, Mtb-MDP1, and ML-LBP. After reaction for 30 min, DNA was extracted, fractionated with gel electrophoresis and visualized by UV light after staining with ethidium bromide. M, marker. N, nicked DNA. S, supercoiled DNA.
doi:10.1371/journal.pone.0020985.g006

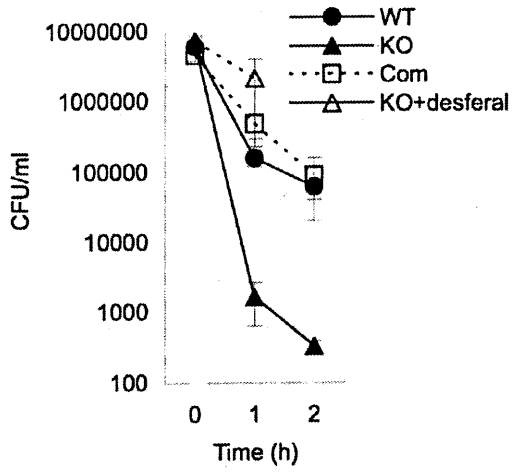

Figure 7. MDP1-deficient *M. smegmatis* is susceptible to H_2O_2 treatment. Bacteria at an exponential growth phase were treated with 12.5 mM H_2O_2 and the survival rate was determined by CFU. Closed circle, the wild-type *M. smegmatis* (WT). Closed triangle, MDP1-deficient *M. smegmatis* (KO), Open square, Ms-MDP1-complemented strain (Com). Open triangle, the MDP1-deficient strain pretreated with 40 mM desferal to confirm that iron is involved in the killing by H_2O_2 treatment (KO+desferal).
doi:10.1371/journal.pone.0020985.g007

from DNase 1 and the Fenton reaction, also support our finding [37]. Our finding on the new type of iron detoxication and storage protein will provide important information on the strategy and insight into virulence of mycobacteria.

Methods

Bacterial strains and proteins

MDP1-deficient *Mycobacterium smegmatis* was a gift from Dr. Thomas Dick [29]. The complemented strain was generated previously [22]. BCG-MDP1 and *M. smegmatis*-MDP1 (Ms-MDP1 or HLP) was purified from cultured BCG Tokyo and *M. smegmatis* mc^2155, respectively, on Sauton media according to the method described previously [17]. Bovine histone H1 and bovine serum albumin (BSA) were purchased from Roche and Sigma, respectively. The open reading flame of MDP1 was amplified from the *M. tuberculosis* H37Rv genome using the following primers, forward: 5′-ccc cat atg aac aaa gca gag ctc att gac-3′, reverse: 5′-ccc aag ctt ttt gcg acc ccg ccg agc gg-3′, containing the restriction sites of NdeI and HindIII. The 645 bp amplicon was cloned into pCR2.1-TOPO (Invitrogen, Carlsbad, CA) and further subcloned as an NdeI-HindIII fragment in the corresponding site of pET-22b (+) (Novagen, Darmstadt, Germany). The plasmid was transformed and expressed in the *Escherichia coli* BL-21 strain and Mtb-MDP1 (Rv2986c) was purified using Ni-NTA agarose (Qiagen, Valencia, CA) with 300 mM imidazole in phosphate buffer (pH 7.4) after obtaining acid soluble proteins [17]. The *M. leprae*-MDP1 (ML-LBP or ML1683) was purified in the same way utilizing a previously constructed expression vector [18]. Concentrations of proteins were determined by Bradford's method [38] using BSA as a standard.

SPR analysis by Biacore biosensor

The interaction between BCG-MDP1 and metal was monitored by measuring SPR using a BIAcore 2000 biosensor (GE Healthcare, Buckinghamshire, UK). All binding reactions were performed at 25°C in 10 mM HEPES buffer, pH 7.4, including 150 mM NaCl, 1% BSA, 3 mM EDTA, and 0.005% surfactant P20 (HBSEP buffer). BCG-MDP1 was immobilized to the dextran matrix on the CM5 sensor chip (GE) using an amine coupling kit according to the manufacturer's instructions (GE). Metals, such as ammonium iron (III) citrate, $CuSO_4$, $MgSO_4$, $MnCl_2$, $ZnSO_4$, and $FeSO_4$, were dissolved in HBSEP buffer to a final metal ion concentration of 1 mM and injected over both the control and BCG-MDP1-immobilized sensor chip.

Detection of MDP1-^{55}Fe interaction

A 96-well ELISA plate (Sumitomo, Tokyo, Japan) was coated overnight with 5 μg/ml BCG-MDP1, Mtb-MDP1, ML-LBP or BSA in borate-buffered saline (pH 9.2) at 4°C. The wells were then washed with phosphate buffered saline (PBS). One hundred μl of PBS containing 1 μCi of $^{55}FeCl_3$ (PerkinElmer, Boston, MA) was added into the wells coated with the proteins. In some cases, $^{55}FeCl_3$ was incubated in 10 mM ascorbic acid for 30 min before addition to the wells. After 30 min incubation, the wells were washed four times in PBS containing 0.05% Tween 20. Then pre-warmed water at 37°C containing 1% SDS and 10 mM cold ammonium iron (III) citrate was added and the wells were flushed by pipetting. Twenty μl of the suspension was then spotted onto Whatman 3 MM paper and its radioactivity was counted by a liquid scintillation counter (Aloka, Tokyo, Japan).

Inductively coupled plasma mass spectrometry (ICP-MS) analysis

After a heparin column was washed out with 10 mM sodium phosphate (pH 7), 1 ml of 0.1 mg/ml BCG-MDP1 or Mtb-MDP1 solution in pure water was incubated for 30 min. After washing, the column was incubated in the presence of 1 mM ammonium iron (III) (1 ml) citrate for 30 min. Unbound iron was washed out and the MDP1-iron complex was eluted by sodium phosphate buffer containing 2 M NaCl. Each sample of approximately 0.1 g was weighed accurately in quartz plates, and they were gradually carbonized with 0.5 ml of sulfuric acid using hot plates. They were then heated for 8 hours at 510°C in an electric furnace and finally washed. After cooling, the residue was dissolved with 1.25 ml of nitric acid and diluted to 25 ml with ultra pure water (the analysis solution). The Fe concentration of each analysis solution was determined by ICP-MS (Model ELAN DRC II; Perkin Elmer). We repeated the experiments 5 and 3 times for BCG-MDP1 and Mtb-MDP1, respectively.

Assay of ferroxidase activity

To determine whether MDP1 converts Fe^{2+} to Fe^{3+} using O_2 as oxidant, 0.4 mM $FeSO_4$ as 15 mM solution at pH 3.5 were added to 1.4 mM MDP1 in 20 mM Tris-HCl (pH 7.0) including with 150 mM NaCl. The protein solution was pre-incubated at 37°C for 10 min. UV spectral absorption at 305 nm has been traditionally used to monitor a μ-oxo-bridged Fe^{3+} dimmers, which was monitored by spectrophotometer U-3000 (HITACHI, Tokyo, Japan). MDP1 produced no UV absorbance in the absence of Fe^{2+}. Lineweaver-Burk plot was used for considering the inverse values of the absorption per 60 s after addition of 0.0125–0.1 mM $FeSO_4$. The Kinetic parameters (K_m) were calculated by direct linear plot through the two points, K_m and V that satisfy the Michaelis-Menten equation exactly for every observation [39]. The best estimates, K_m was taken as the medians of the two sets of estimates.

Monitoring hydroxyl radical generation

Level of hydroxyl radical generation by the Fenton reaction were measured using L-012 (0.08 mM) as a probe as previously described [26]. The total reaction volume was 50 μl containing 20 mM Tris

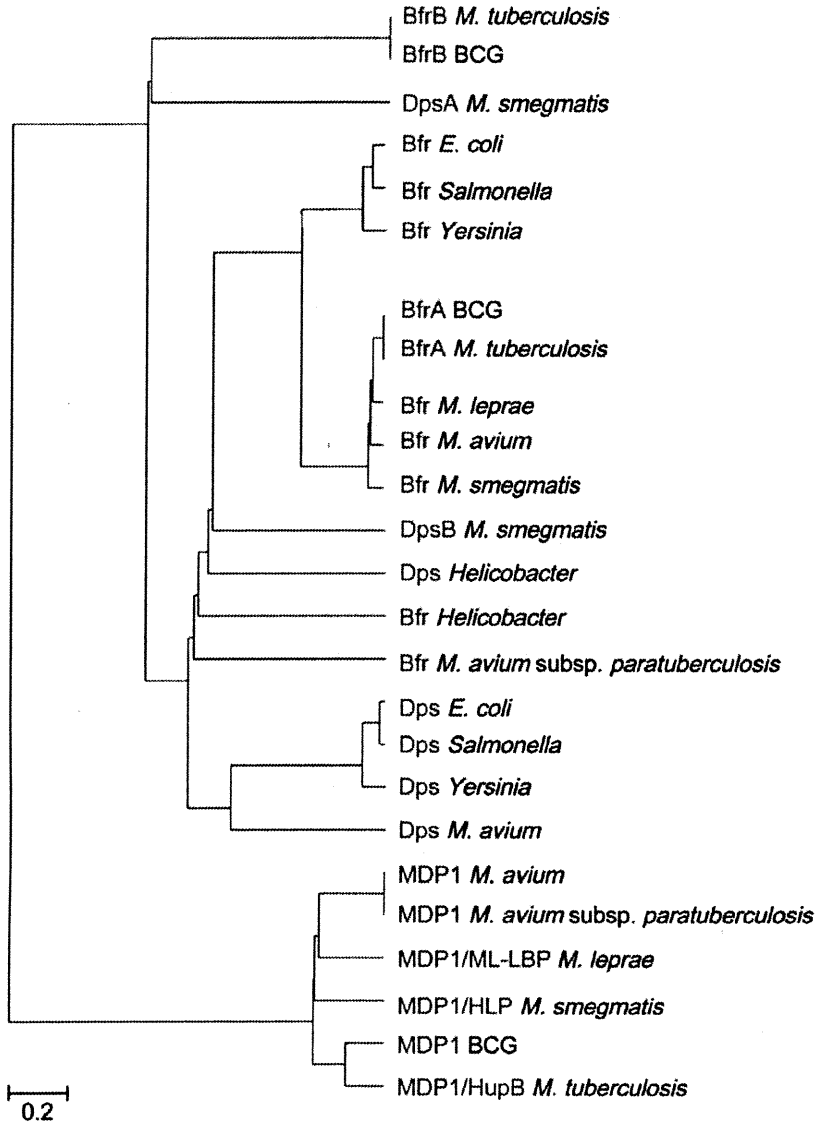

Figure 8. Phylogenetic tree of MDP1/ML-LBP homologues and ferritin superfamily proteins. The amino acid sequences of BCG-MDP1 (AB013441), *M. tuberculosis*-MDP1 (NP_217502), *M. avium*-MDP1 (YP_883003), *M. avium* subsp. *paratuberculosis* -MDP1 (NP_961958), *M. smegmatis*-MDP1 (YP_886729), *M. leprae*-ML-LBP (MDP1) (NP_302157), BCG-bacterioferritin A (BfrA) (YP_978002), BCG-BfrB (YP_979983), *M. tuberculosis*-BfrA (CAB10050), *M. tuberculosis*-BfrB (AAF06357), *M. avium*-Bfr (YP_882020), *M. avium* subsp. *paratuberculosis* (P45430), *M. smegmatis* Bfr (ABK70328), *M. leprae*-Bfr (AAA21339), *E. coli*-Bfr (AP_004454), *Salmonella enterica*-Bfr (CBY97651), *Yersinia pestis*-Bfr (AAS60481), *Helicobacter pylori*-Bfr (CAA06826), *M. avium*-Dps (YP_884099), *M. avium* subsp. *paratuberculosis*-Dps (NP_962494), *M. smegmatis*-DpsA (ABK75435), *M. smegmatis*-DpsB (ABK69831), *E. coli*-Dps (U00096.2), *Salmonella enterica*-Dps (Car32361.1), *Yersinia pestis*-Dps (AL590842.1), and *Helicobacter pylori*-Dps (1JI4_L) are compared by using Genetyx (Ver.16.1) software according to the UPGMA algorism. Values, 0.2, in the figure represent evolutionary distances.
doi:10.1371/journal.pone.0020985.g008

HCl (pH 7.5), 50 mM NaCl. Three μM Histone H1, BCG-MDP1, Mtb-MDP1, and ML-LBP were incubated with 25 or 50 μM $FeSO_4$ and 1 mM H_2O_2. After addition of L-012 (5 μl), CHL intensity was recorded continuously for 20–140 seconds using a Luminescence Reader BLR-201 (Aloka, Tokyo, Japan). The level of hydroxyl radical generation by the combination of 25 or 50 μM $CuSO_4$ and 1 mM H_2O_2 was monitored in the same way.

DNA protection assay

DNA protection from oxidative damage and enzymatic digestion was assessed *in vitro* using pUC19 plasmid DNA (2686 bp, 50 nM), purified by a Qiaprep spin plasmid miniprep kit (Qiagen). The total reaction volume was 20 μl in pure water. Plasmid DNA was allowed to interact with MDP1, ML-LBP, or bovine Histone H1 for 30 min prior to the introduction of 25 or 50 μM $FeSO_4$ and 1 mM H_2O_2 or treatment with 50 or 100 μg/ml DNase I (Sigma, St.Louis, MO). The reaction mixtures were incubated for 30 min at room temperature before the reactions were stopped by incubation with 1% SDS and proteins were degraded by treatment with 20 μg/ml PronaseK (Sigma) for 30 min. Then the plasmid was extracted using phenol-chloroform extraction and 10 μl of sample was loaded on 1% agarose gel in

TAE buffer for electrophoresis. The gel was stained with ethidium bromide and DNA was visualized under UV light.

H_2O_2 treatment

M. smegmatis strains were grown to an OD600 of 0.5 to 0.7 in LB medium at 37°C. The bacterial culture was then diluted to 0.1 OD by the medium for the assay. The reaction was initiated by adding a final concentration of 12.5 mM H_2O_2 and incubated for 0, 1, or 2 hours. If necessary, bacteria were pretreated with 40 mM desferal (Sigma) for 5 min before exposure to H_2O_2. At each time point, the bacterial suspension was serially diluted using sterilized water and plated onto LB agar (Sigma). Living bacteria were enumerated by counting CFU after incubation at 37°C for 4–6 days.

Supporting Information

Figure S1 MDP1/ML-LBP homologues. Blast search was performed for amino acid sequence of BCG-MDP1 against all protein database using the National Center for Biotechnology Information's (NCBI) BLAST server and proteins with over 150 of total score are aligned. Conserved domain of Integration host factor (IHF) and HU were shown by yellow box, which was identified with domain search using NCBI server. MDP1-specific DNA binding region [20] that interacts with GC-rich DNA was indicated by red.
(DOC)

Figure S2 Ferroxidase activity of Ms-MDP1. The conversion from Fe^{2+} to Fe^{3+} was scanned by measuring the absorbance at 305 nm. Black line, 0.4 mM $FeSO_4$; blue line, 0.4 mM $FeSO_4$+1.4 μM Histone H1; red line, 0.4 mM $FeSO_4$+1.4 μM Ms-MDP1.
(TIF)

Figure S3 Ferroxidase activity of Mtb-MDP1 and ferritin using hydroxyl peroxide, as the oxidant The conversion from Fe^{2+} to Fe^{3+} was monitored by spectral analysis at 305 nm. Hydroxyl peroxide (6–108 mM) were added to the solution of either 0.5 μM Mtb-MDP1 (A) or horse ferritin (B) including with 21 μM $FeSO_4$.
(TIF)

Acknowledgments

We are grateful to Dr. Thomas Dick, Novartis Institute for Tropical Diseases, for providing Ms-MDP1/HLP-KO *M. smegmatis*. We also thank Sara Matsumoto for assistance with the experiments and heartfelt encouragement.

Author Contributions

Conceived and designed the experiments: MT MO-O MI KI TA HO K. Kobayashi AR SM. Performed the experiments: MT MO-O EFS K. Kitadokoro YN MYN YS SM. Analyzed the data: MT MO-O MI KI TA HO K. Kobayashi AR SM. Wrote the paper: MT MO-O EFS K. Kobayashi AR SM.

References

1. Chiancone E, Ceci P, Ilari A, Ribacchi F, Stefanini S (2004) Iron and proteins for iron storage and detoxification. Biometals 17: 197–202.
2. Banyard SH, Stammers DK, Harrison PM (1978) Electron density map of apoferritin at 2.8-A resolution. Nature 271: 282–284.
3. Carrondo MA (2003) Ferritins, iron uptake and storage from the bacterioferritin viewpoint. EMBO J 22: 1959–1968.
4. Bozzi M, Mignogna G, Stefanini S, Barra D, Longhi C, et al. (1997) A novel non-heme iron-binding ferritin related to the DNA-binding proteins of the Dps family in Listeria innocua. J Biol Chem 272: 3259–3265.
5. Ilari A, Stefanini S, Chiancone E, Tsernoglou D (2000) The dodecameric ferritin from Listeria innocua contains a novel intersubunit iron-binding site. Nat Struct Biol 7: 38–43.
6. Bou-Abdallah F, Lewin AC, Le Brun NE, Moore GR, Chasteen ND (2002) Iron detoxification properties of Escherichia coli bacterioferritin. Attenuation of oxyradical chemistry. J Biol Chem 277: 37064–37069.
7. Cirillo SL, Subbian S, Chen B, Weisbrod TR, Jacobs WR, Jr., et al. (2009) Protection of *Mycobacterium tuberculosis* from reactive oxygen species conferred by the mel2 locus impacts persistence and dissemination. Infect Immun 77: 2557–2567.
8. Boelaert JR, Vandecasteele SJ, Appelberg R, Gordeuk VR (2007) The effect of the host's iron status on tuberculosis. J Infect Dis 195: 1745–1753.
9. De Voss JJ, Rutter K, Schroeder BG, Su H, Zhu Y, et al. (2000) The salicylate-derived mycobactin siderophores of *Mycobacterium tuberculosis* are essential for growth in macrophages. Proc Natl Acad Sci USA 97: 1252–1257.
10. Barry CE, 3rd, Boshoff H (2005) Getting the iron out. Nat Chem Biol 1: 127–128.
11. Gold B, Rodriguez GM, Marras SA, Pentecost M, Smith I (2001) The *Mycobacterium tuberculosis* IdeR is a dual functional regulator that controls transcription of genes involved in iron acquisition, iron storage and survival in macrophages. Mol Microbiol 42: 851–865.
12. Gupta V, Gupta RK, Khare G, Salunke DM, Tyagi AK (2009) Crystal structure of Bfr A from *Mycobacterium tuberculosis*: incorporation of selenomethionine results in cleavage and demetallation of haem. PLoS One 4: e8028.
13. Pessolani MC, Smith DR, Rivoire B, McCormick J, Hefta SA, et al. (1994) Purification, characterization, gene sequence, and significance of a bacterioferritin from *Mycobacterium leprae*. J Exp Med 180: 319–327.
14. Cole ST, Eiglmeier K, Parkhill J, James KD, Thomson NR, et al. (2001) Massive gene decay in the leprosy bacillus. Nature 409: 1007–1011.
15. Cole ST, Brosch R, Parkhill J, Garnier T, Churcher C, et al. (1998) Deciphering the biology of *Mycobacterium tuberculosis* from the complete genome sequence. Nature 393: 537–544.
16. Colangeli R, Haq A, Arcus VL, Summers E, Magliozzo RS, et al. (2009) The multifunctional histone-like protein Lsr2 protects mycobacteria against reactive oxygen intermediates. Proc Natl Acad Sci USA 106: 4414–4418.
17. Matsumoto S, Yukitake H, Furugen M, Matsuo T, Mineta T, et al. (1999) Identification of a novel DNA-binding protein from *Mycobacterium bovis* bacillus Calmette-Guerin. Microbiol Immunol 43: 1027–1036.
18. Shimoji Y, Ng V, Matsumura K, Fischetti VA, Rambukkana A (1999) A 21-kDa surface protein of *Mycobacterium leprae* binds peripheral nerve laminin-2 and mediates Schwann cell invasion. Proc Natl Acad Sci USA 96: 9857–9862.
19. Aoki K, Matsumoto S, Hirayama Y, Wada T, Ozeki Y, et al. (2004) Extracellular mycobacterial DNA-binding protein 1 participates in *Mycobacterium*-lung epithelial cell interaction through hyaluronic acid. J Biol Chem 279: 39798–39806.
20. Furugen M, Matsumoto S, Matsuo T, Matsumoto M, Yamada T (2001) Identification of the mycobacterial DNA-binding protein 1 region which suppresses transcription in vitro. Microb Pathog 30: 129–138.
21. Matsumoto S, Matsumoto M, Umemori K, Ozeki Y, Furugen M, et al. (2005) DNA augments antigenicity of mycobacterial DNA-binding protein 1 and confers protection against *Mycobacterium tuberculosis* infection in mice. J Immunol 175: 441–449.
22. Katsube T, Matsumoto S, Takatsuka M, Okuyama M, Ozeki Y, et al. (2007) Control of cell wall assembly by a histone-like protein in Mycobacteria. J Bacteriol 189: 8241–8249.
23. Matsumoto S, Furugen M, Yukitake H, Yamada T (2000) The gene encoding mycobacterial DNA-binding protein I (MDPI) transformed rapidly growing bacteria to slowly growing bacteria. FEMS Microbiol Lett 182: 297–301.
24. Davis TM, Wilson WD (2000) Determination of the refractive index increments of small molecules for correction of surface plasmon resonance data. Anal Biochem 284: 348–353.
25. Hesse L, Beher D, Masters CL, Multhaup G (1994) The beta A4 amyloid precursor protein binding to copper. FEBS Lett 349: 109–116.
26. Imada I, Sato EF, Miyamoto M, Ichimori Y, Minamiyama Y, et al. (1999) Analysis of reactive oxygen species generated by neutrophils using a chemiluminescence probe L-012. Anal Biochem 271: 53–58.
27. Sassetti CM, Boyd DH, Rubin EJ (2003) Genes required for mycobacterial growth defined by high density mutagenesis. Mol Microbiol 48: 77–84.
28. Lewin A, Baus D, Kamal E, Bon F, Kunisch R, et al. (2008) The mycobacterial DNA-binding protein 1 (MDP1) from *Mycobacterium bovis* BCG influences various growth characteristics. BMC Microbiol 8: 91.
29. Lee BH, Murugasu-Oei B, Dick T (1998) Upregulation of a histone-like protein in dormant *Mycobacterium smegmatis*. Mol Gen Genet 260: 475–479.
30. Brooks BW, Young NM, Watson DC, Robertson RH, Sugden EA, et al. (1991) *Mycobacterium paratuberculosis* antigen D: characterization and evidence that it is a bacterioferritin. J Clin Microbiol 29: 1652–1658.
31. Inglis NF, Stevenson K, Hosie AH, Sharp JM (1994) Complete sequence of the gene encoding the bacterioferritin subunit of Mycobacterium avium subspecies silvaticum. Gene 150: 205–206.

32. Janowski R, Auerbach-Nevo T, Weiss MS (2008) Bacterioferritin from Mycobacterium smegmatis contains zinc in its di-nuclear site. Protein Sci 17: 1138–1150.
33. Soares de Lima C, Zulianello L, Marques MA, Kim H, Portugal MI, et al. (2005) Mapping the laminin-binding and adhesive domain of the cell surface-associated Hlp/LBP protein from *Mycobacterium leprae*. Microbes Infect 7: 1097–1109.
34. Gobin J, Horwitz MA (1996) Exochelins of *Mycobacterium tuberculosis* remove iron from human iron-binding proteins and donate iron to mycobactins in the *M. tuberculosis* cell wall. J Exp Med 183: 1527–1532.
35. Gobin J, Moore CH, Reeve JR, Jr., Wong DK, Gibson BW, et al. (1995) Iron acquisition by *Mycobacterium tuberculosis*: isolation and characterization of a family of iron-binding exochelins. Proc Natl Acad Sci USA 92: 5189–5193.
36. Andrews SC, Robinson AK, Rodriguez-Quinones F (2003) Bacterial iron homeostasis. FEMS Microbiol Rev 27: 215–237.
37. Farhana A, Kumar S, Rathore SS, Ghosh PC, Ehtesham NZ, et al. (2009) Mechanistic insights into a novel exporter-importer system of *Mycobacterium tuberculosis* unravel its role in trafficking of iron. PLoS One 3: e2087.
38. Bradford MM (1976) A rapid and sensitive method for the quantitation of microgram quantities of protein utilizing the principle of protein-dye binding. Anal Biochem 72: 248–254.
39. Eisenthal R, Cornish-Bowden A (1974) The direct linear plot. A new graphical procedure for estimating enzyme kinetic parameters. Biochem J 139: 715–720.

Vaccine 29 (2011) 6881–6887

Contents lists available at ScienceDirect

Vaccine

journal homepage: www.elsevier.com/locate/vaccine

Loss of anti-mycobacterial efficacy in mice over time following vaccination with *Mycobacterium bovis* bacillus Calmette-Guérin

Yuriko Ozeki[a,b,*], Yukio Hirayama[a], Takemasa Takii[c], Saburo Yamamoto[d], Kazuo Kobayashi[e], Sohkichi Matsumoto[a,**]

[a] Department of Bacteriology, Osaka City University Graduate School of Medicine, 1-4-3 Asahimachi, Abeno-ku, Osaka 545-8585, Japan
[b] Department of Food and Nutrition, Sonoda Women's University, 7-29-1 Minamitsukaguchi-cho, Amagasaki, Hyogo, Japan
[c] Department of Molecular Health Sciences, Graduate School of Pharmaceutical Sciences, Nagoya City University, 3-1 Tanabe, Mizuho, Nagoya 467-8603, Japan
[d] Japan BCG Central Laboratory, 3-1-5 Matsuyama, Kiyose, Tokyo 204-0022, Japan
[e] Department of Immunology, National Institute of Infectious Diseases, 1-23-1 Toyama, Shinjuku-ku, Tokyo 162-8640, Japan

ARTICLE INFO

Article history:
Received 30 April 2011
Received in revised form 10 July 2011
Accepted 16 July 2011
Available online 29 July 2011

Keywords:
Mycobacterium
Vaccine
Adult pulmonary tuberculosis
BCG
Cellular immunity
TH1

ABSTRACT

Mycobacterium bovis bacillus Calmette-Guérin (BCG) is the most often used vaccine worldwide and sole vaccine against tuberculosis. BCG is protective against severe form of childhood tuberculosis but less or not protective to adult pulmonary tuberculosis. Therefore, improved vaccination strategies and development of new tuberculosis vaccines are urgent demands. For those purposes, appropriate animal models that reflect human are critically useful. However, in animal models, BCG vaccination protects well against subsequent challenge of *Mycobacterium tuberculosis*. In this study we evaluated the duration of protective efficacy of the BCG vaccination in mice over time and found that efficacy was diminished 40 weeks after vaccination. The aged mice older than 45 weeks are protected sufficiently after the vaccination with BCG, suggesting that loss of its efficacy is not dependent on the age of mice but rather depends on the period from vaccination. The loss of protection occurred in TH1 polarized STAT6 deficient mice despite the maintenance of interferon (IFN)-gamma production activity of lymph node cells and splenic $CD4^+$ T cells against *M. tuberculosis* antigens. Our data suggest that the duration from vaccination may explain the variation in BCG efficacy against adult pulmonary tuberculosis.

1. Introduction

Tuberculosis remains a serious threat for human health worldwide, where around 9.4 million people develop tuberculosis and 1.8 million people die each year [1].

Mycobacterium bovis bacillus Calmette-Guérin (BCG) is an attenuated strain of *M. bovis* [2] and the only currently available vaccine against tuberculosis. Nowadays it is accepted that BCG is effective for severe forms of childhood tuberculosis, such as disseminated tuberculosis and meningitis, but the efficacy for pulmonary tuberculosis in adults is variable among different populations and studies [3], and ineffectiveness was reported by controlled trials of over one hundred thousand people in India [2]. Poor or lack of efficacy of BCG for adult pulmonary tuberculosis is a serious problem in controlling the disease [2,4], because many deaths from tuberculosis are caused in adults and pulmonary tuberculosis is the most frequent clinical entity of tuberculosis. Several factors, such as strain variation [5], immune disturbance by exposure to environmental mycobacteria [6], and methodological discrepancies [7], are thought to be involved in the variation of effectiveness of BCG for adult pulmonary tuberculosis. In addition, decline of BCG efficacy with time was reported in human studies [8,9], implying that the duration of time from vaccination is related with the poor effectiveness of BCG in adult tuberculosis, although one study reported that it maintains over 50 years after vaccination [10].

In animal models, including mice, BCG vaccination induces a remarkable protection against subsequent challenge with *M. tuberculosis*. IFN-gamma is considered as a key cytokine [11–13] and IFN-gamma-producing $CD4^+$ T-helper 1 cells (TH1) play a pivotal role in the acquired protective immunity induced by BCG vaccination. In addition, the importance of IFN-gamma signaling pathways, such as the mutation of interferon-gamma receptors, in defense against mycobacterial infection is demonstrated by human studies [14,15].

Abbreviations: APCs, antigen-presenting cells; BCG, *Mycobacterium bovis* bacillus Calmette-Guérin; CFUs, colony forming units; KM, kanamycin; TH1, type 1 $CD4^+$ T-helper cells; TH2, type 2 $CD4^+$ T-helper cells.

* Corresponding author at: Department of Bacteriology, Osaka City University Graduate School of Medicine, 1-4-3 Asahi-machi, Abeno-ku, Osaka 545-8585, Japan. Tel.: +81 6 6645 3746; fax: +81 6 6645 3747.
** Corresponding author. Tel.: +81 6 6645 3746; fax: +81 6 6645 3747.
E-mail addresses: yuriozeki@med.osaka-cu.ac.jp (Y. Ozeki), sohkichi@med.osaka-cu.ac.jp (S. Matsumoto).

0264-410X/$ – see front matter © 2011 Elsevier Ltd. All rights reserved.
doi:10.1016/j.vaccine.2011.07.051

The aim of this study was to clarify the efficacious duration of BCG vaccination and immune responses in mice vaccinated with BCG. Although it is believed that BCG always confers protection against subsequent challenge of mycobacteria in animal models, we found that BCG efficacy was diminished 40 weeks after vaccination. The decline of protection is dependent on the time after BCG vaccination but not the age of mice. The loss of protection occurred even while maintaining IFN-gamma-productivity by $CD4^+$ T cells upon stimulation with *M. tuberculosis* antigens. Our data suggest the duration of time from vaccination may influence the variability of BCG efficacy against adult pulmonary tuberculosis.

2. Materials and methods

2.1. Animals

Female C57BL/6 and BALB/c mice were purchased from SLC (Shizuoka, Japan). STAT6-deficient BALB/c mice were purchased from the Jackson Laboratory (Bar Harbor, ME) and bred and maintained. Female C57BL/6, STAT6-deficient, and BALB/c mice of 6–8-weeks-old were used in the experiments. For the analysis of age effects in vaccination, we used female C57BL/6 mice aged 45–55 weeks old. Experiments were conducted according to the standard guidelines for animal experiments of Osaka City University Graduate School of Medicine.

2.2. BCG vaccination and challenge with kanamaycin-resistant BCG

C57BL/6, BALB/c, and STAT6-deficient mice were vaccinated via the peritoneal route with 10^5 colony-forming units (CFUs) of BCG suspended in 100 μL of sterilized phosphate-buffered saline (PBS). At various times after vaccination, lungs, livers, and spleens were homogenized in 1 mL sterile distilled water and serial dilutions were plated on Middlebrook 7H11 agar containing oleic acid, dextrose, albumin, and catalase enrichment (Difco) (7H11-OADC agar). CFUs were counted after culturing at 37 °C for 20–30 days. In some experiments, mice were intratracheally challenged with $5 \times 10^{4-5}$ CFUs of kanamycin (KM) resistant BCG suspended in 50 μL of PBS at 3, 20, and 40 weeks postvaccination. Five weeks later, lungs were homogenized as described above and serial dilutions of homogenates were plated on 7H11-OADC agar containing 10 μg/mL of KM.

2.3. Culture of lymph node cells and $CD4^+$ T cells in vitro

Axillary lymph nodes were obtained from at least three mice per group and single cell suspensions were prepared in Hanks' balanced salt solution by gently teasing the nodes between the frosted ends of two glass slides. This procedure routinely provided single cell suspensions with 90–95% viability as assessed by trypan blue dye exclusion. Lymph node cells were cultured in RPMI 1640 medium containing 10% heat-inactivated fetal calf serum, 2 mM L-glutamine, 100 U/mL penicillin and 100 μg/mL streptomycin (Life Technologies, Grand Island, NY). In some experiments, $CD4^+$ T cells were isolated from mice using a $CD4^+$ T Cell Isolation Kit (Miltenyl Biotec, Bergisch Gladgach, Germany) after erythrocyte depletion using 0.83% ammonium chloride solution. Obtained cells were labeled with PE-conjugated anti-CD4 mAb (eBioscience) and analyzed by flow cytometry. The purity of selected populations was confirmed as >96%. Non-$CD4^+$ cells retained in elution were incubated for over 2 h. Attached cells were used as antigen-presenting cells (APCs) after irradiation (20 Gy).

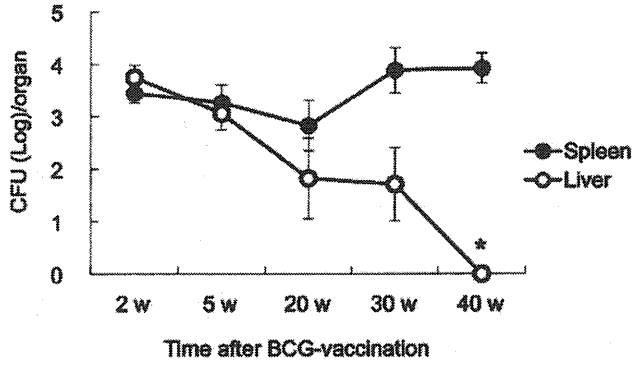

Fig. 1. Time course of surviving BCG number after vaccination. C57BL/6 mice were intraperitoneally vaccinated with 10^5 CFU of BCG. Various times after vaccination, bacterial numbers in livers (open circles) and spleens (closed circles) were monitored. Data represent mean values ± SD for 3–5 mice per group. *$P < 0.05$ versus CFU at 2 weeks after vaccination.

2.4. In vitro T-cell proliferation assay and measurement of cytokine secretion

Lymph nodes cells were resuspended at 2.5×10^6 cells/mL, $CD4^+$ T cells at 6×10^5 cells/mL and APCs at 2×10^5 cells/mL. Cells were cultured for 5 or 7 days with or without 10 μg/mL of purified protein derivatives (PPD, Japan BCG Laboratory, Tokyo) in 96-well plates in RPMI 1640 supplemented with 10% fetal calf serum (FCS), 2 mM L-glutamine, penicillin (100 U/mL), streptomycin (100 μg/mL) and 50 mM 2-mercaptoethanol. Proliferation was evaluated by pulsing the cells with 1 μCi (37 kBq)/well ^3H thymidine for 6 h and measuring ^3H thymidine incorporation using a scintillation counter. Production of IFN-gamma, interleukin (IL)-4, IL-5, and IL-10 in the culture supernatant was measured using commercially available ELISA kits (R&D System, Minneapolis, MN).

2.5. Statistical analysis

Results were analyzed by one-way analysis of variance (ANOVA) using SAS system R.8.1. Data were expressed as mean values ± standard deviation (SD) and considered significant if $P < 0.05$.

3. Results

3.1. Loss of protection induced by BCG vaccination in mice

Anti-tuberculosis immunity can be induced by vaccination with viable but not dead BCG [11,16]. First, in order to know if the survival rate of inoculated BCG correlated with protection, we examined how long BCG is sustained *in vivo*. We inoculated 10^5 CFU of BCG into C57BL/6 mice intraperitoneally and counted bacterial CFUs in organs, such as spleens, livers, and lungs. Although BCG was almost undetectable in lungs during experiments, substantial numbers of BCG were found in both the spleens and livers (Fig. 1). In livers, BCG was gradually eliminated and almost undetectable 40 weeks after vaccination. By contrast, bacterial numbers were unchanged from 2 to 40 weeks after vaccination in spleens.

We next examined the efficacy of BCG vaccination at 20 and 40 weeks postvaccination. Mice were challenged intratracheally with KM-resistant BCG. After 5 weeks, mice were sacrificed and CFUs of KM-resistant BCG in the lungs determined. We found that reduced numbers of CFUs in BCG-vaccinated mice comparing to that in unvaccinated mice at 20 weeks postvaccination. However, we could not find a reduction in CFUs in vaccinated mice at 40 weeks postvaccination (Fig. 2). The protective efficacy of BCG was evident 20 weeks after the vaccination but was lost at 40 weeks

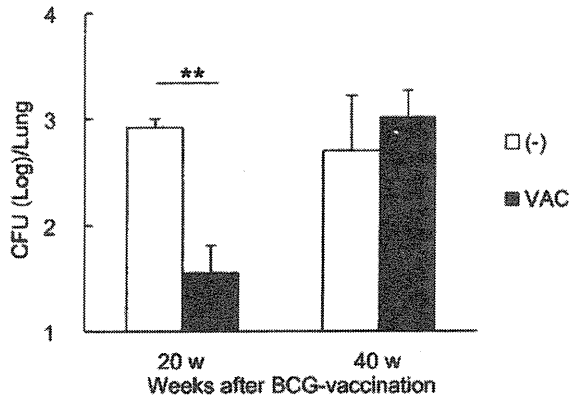

Fig. 2. Influence of time after vaccination on BCG-induced protection in C57BL/6 mice. Twenty or 40 weeks after BCG vaccination, C57BL/6 mice vaccinated with BCG (closed columns) or not (open columns) were intratracheally challenged with 5×10^4 of KM resistant BCG. Five weeks later, mice were sacrificed and CFUs of KM resistant BCG in lungs were counted. $^{**}P < 0.01$ versus unvaccinated mice. Data represent mean values ± SD for 4–6 mice per group.

after vaccination. The experiments were repeated twice, and the loss of protection at 40 weeks postvaccination was reproducibly observed (data not shown).

In order to know the precise mechanism of BCG efficacy, we examined helper T (TH) cell cytokine patterns. TH1 immune responses, such as the production of IFN-gamma, are protective against mycobacterial infection, whereas type 2 helper T cell (TH2) responses, such as production of IL-4 and IL-5, are not [17,18]. To clarify the mechanism of BCG efficacy, we examined cytokine responses of lymph node cells against *M. tuberculosis* antigens, PPD, at 20 and 40 weeks postvaccination. High levels of IFN-gamma production were observed when lymph node cells derived from mice 20, but not 40, weeks after vaccination were incubated with PPD (Fig. 3A). By contrast, significant production of both IL-4 and IL-5 was observed when lymph node cells derived from mice at 40 weeks postvaccination were incubated with PPD (Fig. 3B and C).

3.2. BCG induces protection in aged mice

In order to clarify the participation of age factors in the decline of protection induced by BCG vaccination, we studied BCG efficacy using aged mice. Young (5 weeks old) and aged (45–55 weeks old) C57BL/6 mice were intraperitoneally vaccinated with 10^5 CFUs of BCG. Mice were then challenged with KM-resistant BCG and protection was assessed by comparing CFUs of KM-resistant BCG in the lungs at 5 weeks postchallenge (Fig. 4A). Significantly reduced numbers of CFUs were seen in both BCG-vaccinated young and aged mice comparing to unvaccinated controls, showing that BCG vaccination can induce protection in mice aged 45–55 weeks. Simultaneously, we studied cytokine responses of lymph node cells. Lymph node cells derived from aged mice prevaccinated with BCG produced comparable amounts of IFN-gamma to young mice, when stimulated with PPD (Fig. 4B). The $CD4^+$ splenic T cells produced similar levels of IFN-gamma when stimulated with PPD as lymph node cells (data not shown).

3.3. Protection is lost despite maintenance of TH1 responses to PPD

We next examined whether the loss of BCG effectiveness observed in C57BL/6 mice occurred in another mouse strain, BALB/c. In C57BL/6 mice, we observed impaired TH1 and strengthened TH2 responses of lymph node cells to PPD when protection was diminished (Fig. 3). We considered this shift of immune

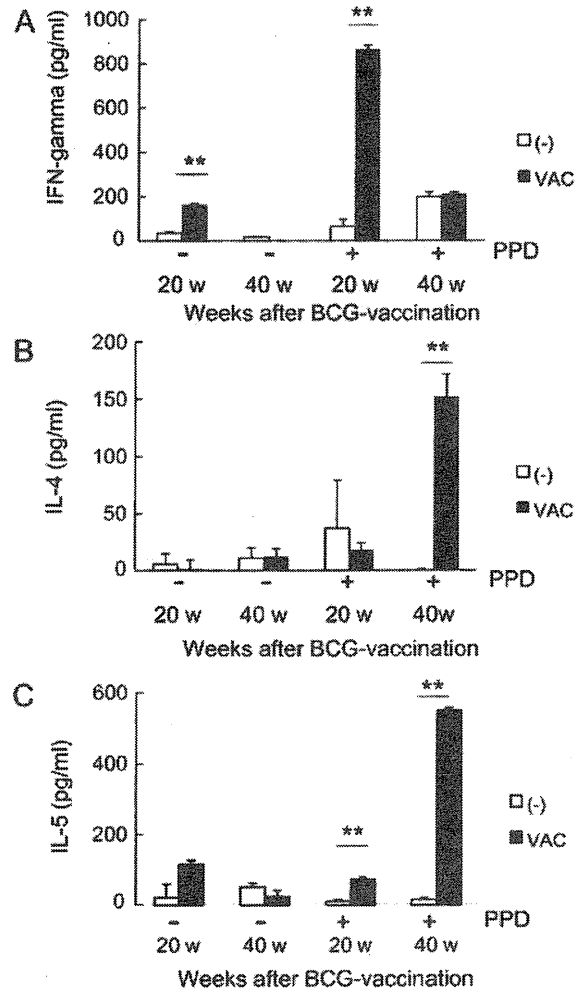

Fig. 3. Cytokine production from lymph node cells after stimulation with *M. tuberculosis* antigens, PPD *in vitro*. Lymph nodes cells (2.5×10^6 cells/ml) derived from BCG-vaccinated (closed columns) or unvaccinated (open columns) mice were cultured with or without 10 μg/ml of PPD for 7 days. The amounts of IFN-gamma (A), IL-4 (B), and IL-5 (C) in the supernatants were determined by ELISA. $^*P < 0.05$, $^{**}P < 0.01$ versus unvaccinated mice.

response from TH1 to TH2 to mycobacterial antigens might cause loss of protection. To examine this hypothesis as well, we used STAT6 deficient BALB/c mice previously constructed [19]. STAT6 is a transcription factor that translocates to the cell nucleus after phosphorylation and plays a central role in IL-4 mediated biological function [20,21]. Robust TH1 and impaired TH2 responses are reported in STAT6 knockout mice [20,21].

Wild-type BALB/c and STAT6 knockout mice were vaccinated with 10^5 CFU BCG intraperitoneally and viable numbers of BCG in spleens and liver were counted (Fig. 5A and B). In spleens, 10^4–10^5 CFUs of BCG continuously remained in both wild type and STAT6 knockout BALB/c mice until 40 weeks after vaccination (Fig. 5A). As observed in C57BL/6 mice, both mice showed a gradual decrease of inoculated BCG in the liver (Fig. 5B).

We next examined TH1 responses to PPD in STAT6 knockout mice after BCG vaccination. Twenty and 40 weeks after vaccination, we analyzed the responses of lymph node cells (Fig. 6) and $CD4^+$ T cells to PPD *in vitro*. T cells of STAT6-knockout mice showed significantly higher levels of proliferation when compared to control mice at both 20 and 40 weeks postvaccination (Fig. 6A). Significantly higher levels of IFN-gamma production were detected from lymph node cells of STAT6 knockout mice compared to wild type

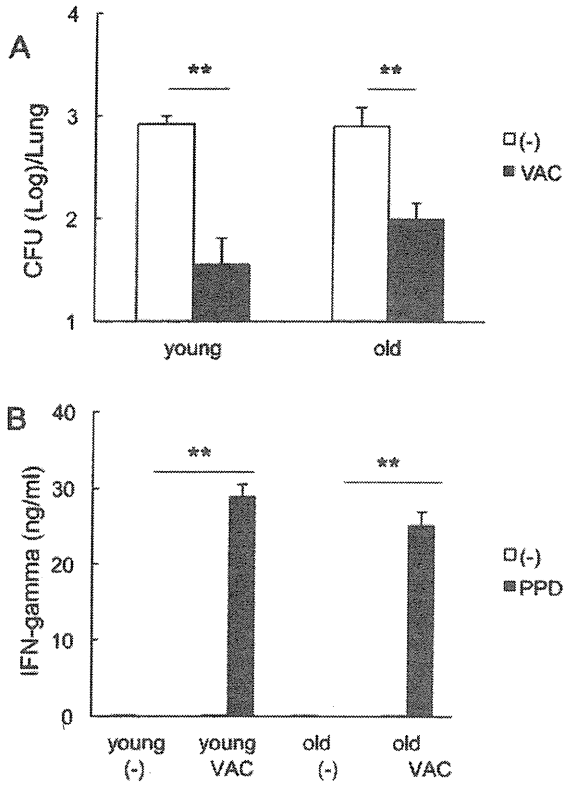

Fig. 4. Effect of BCG vaccination in aged C57BL/6 mice. Young (5 weeks old) and aged (45–55 weeks olds) mice were vaccinated with BCG. Five weeks after vaccination, mice were intratracheally challenged with KM resistant BCG and sacrificed at 5 weeks postchallenge. Living bacterial numbers in vaccinated (closed column) or unvaccinated (open column) mouse lungs were counted (A). Five weeks after vaccination, 2.5×10^6 lymph node cells were cultured with (closed columns) or without (open columns) of 10 μg/ml of PPD for 7 days. The levels of IFN-gamma in culture supernatants were determined by ELISA (B). Data represent mean values ± SD for 6 mice per group in (A). $^{**}P < 0.01$ versus unvaccinated mice in both (A) and (B).

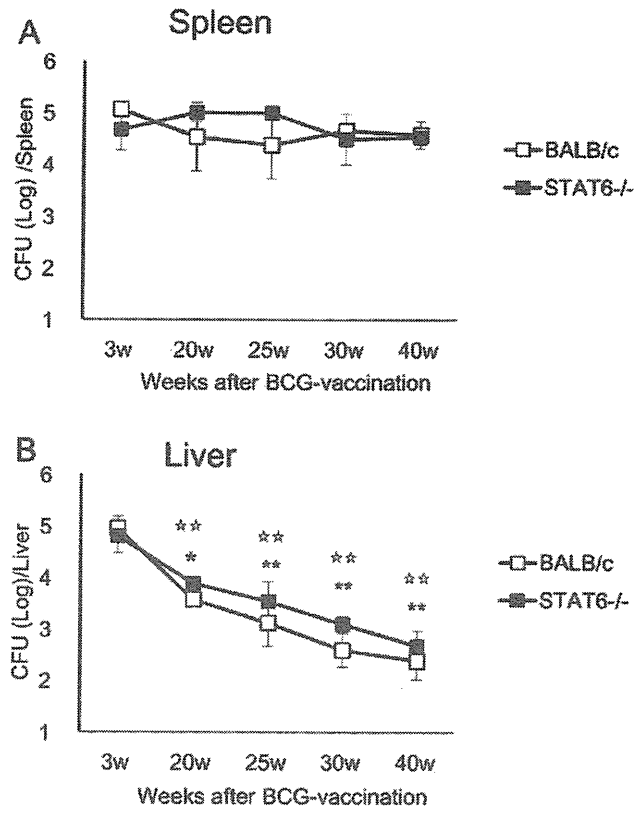

Fig. 5. Survival of BCG in BALB/c and STAT6 knockout mice after vaccination. BALB/c and STAT6 knockout mice were intraperitoneally vaccinated with 10^5 CFU of BCG. At various times after vaccination, bacterial numbers in the spleen (A) and liver (B) of BALB/c (open squares) or STAT6 knockout (closed squares) mice were counted after plating serially diluted lung homogenates on 7H11-OADC agar. Data represent mean values ± SD for 4–5 mice per group. $^{**}P < 0.01$ versus CFU of BALB/c mice at 3 weeks after vaccination. $^{**}P < 0.01$; $^{*}P < 0.05$ versus CFU of STAT 6 knockout mice at 3 weeks after vaccination.

mice at both 20 and 40 weeks postvaccination (Fig. 6B). The reduction of IFN-gamma responses to PPD observed in wild type C57BL/6 (Fig. 3A) at 40 weeks after infection was not seen in STAT6 knockout mice or wild type mice (Fig. 6B). We obtained similar results when using splenic $CD4^+$ T cells and APCs (data not shown).

Simultaneously, we analyzed TH2 cytokine production in cultured supernatants. We could detect IL-4 production from lymph node cells when those were stimulated with PPD at both time points. The level of IL-4 was significantly lower in STAT6 knockout than wild type mice at both time points (Fig. 6C). By contrast, small amount of IL-5 production (213 ± 6.5 pg/ml) was seen when lymph node cells derived from wild type but not STAT6 knockout mice at 20 weeks after vaccination (data not shown). Lymph node cells derived from neither wild type nor STAT6 knockout mice at 40 weeks after vaccination produced IL-5 upon stimulated with PPD (data not shown). Taken together, in BALB/c mice, the TH1 immune response to PPD was maintained and in STAT6 knockout mice, the TH1 polarized immune response was maintained until 40 weeks postvaccination.

Finally we addressed whether the protective effects of BCG vaccination is maintained in TH1 polarized STAT6 knockout mice. Mice vaccinated with BCG or given saline were intratracheally challenged with KM-resistant BCG at 3, 20 and 40 weeks postvaccination. We accessed the protective effects by comparing CFUs of KM-resistant BCG in the lungs (Fig. 7). We found significantly reduced CFUs in BCG-vaccinated mice compared to unvaccinated mice at both 3 and 20 weeks postvaccination (Fig. 7A and B). As seen in the experiments using C57BL/6 mice, impairment of protection was seen in BALB/c mice at 40 weeks postvaccination (Fig. 7C). We also found loss of the protective effects of BCG vaccination in STAT6 knockout mice 40 weeks after vaccination (Fig. 7C).

4. Discussion

Poor effectiveness of the BCG vaccine is a serious matter in controlling tuberculosis [3]. There is an urgent demand to develop novel vaccination strategies or vaccines against tuberculosis. In order to understand the mechanism behind the poor effectiveness of BCG and to evaluate novel vaccine candidates, animal models are critically useful. However, it was thought that BCG vaccination provides good protection from mycobacterial infection in animal models. Accordingly, the usefulness of animal models for developing tuberculosis vaccines has been questioned, because they do not seem to reflect poor protective efficacy of BCG against adult pulmonary tuberculosis. In this study, we showed that efficacy of BCG is lost over time following vaccination in both C57BL/6 and BALB/c mice (Figs. 2 and 7). In these mice adaptive immunity differently respond to some intracellular pathogens such as *Leishmania* and *Yersinia* [22,23]. In such infections, C57BL/6 mice mount strong TH1-type responses, whereas BALB/c mice preferentially activate TH2-type responses, leading different infectious outcomes [22,23]. In contrast, TH1 type immune responses similarly occur in mycobacterial infection in both mouse strains, although C57BL/6

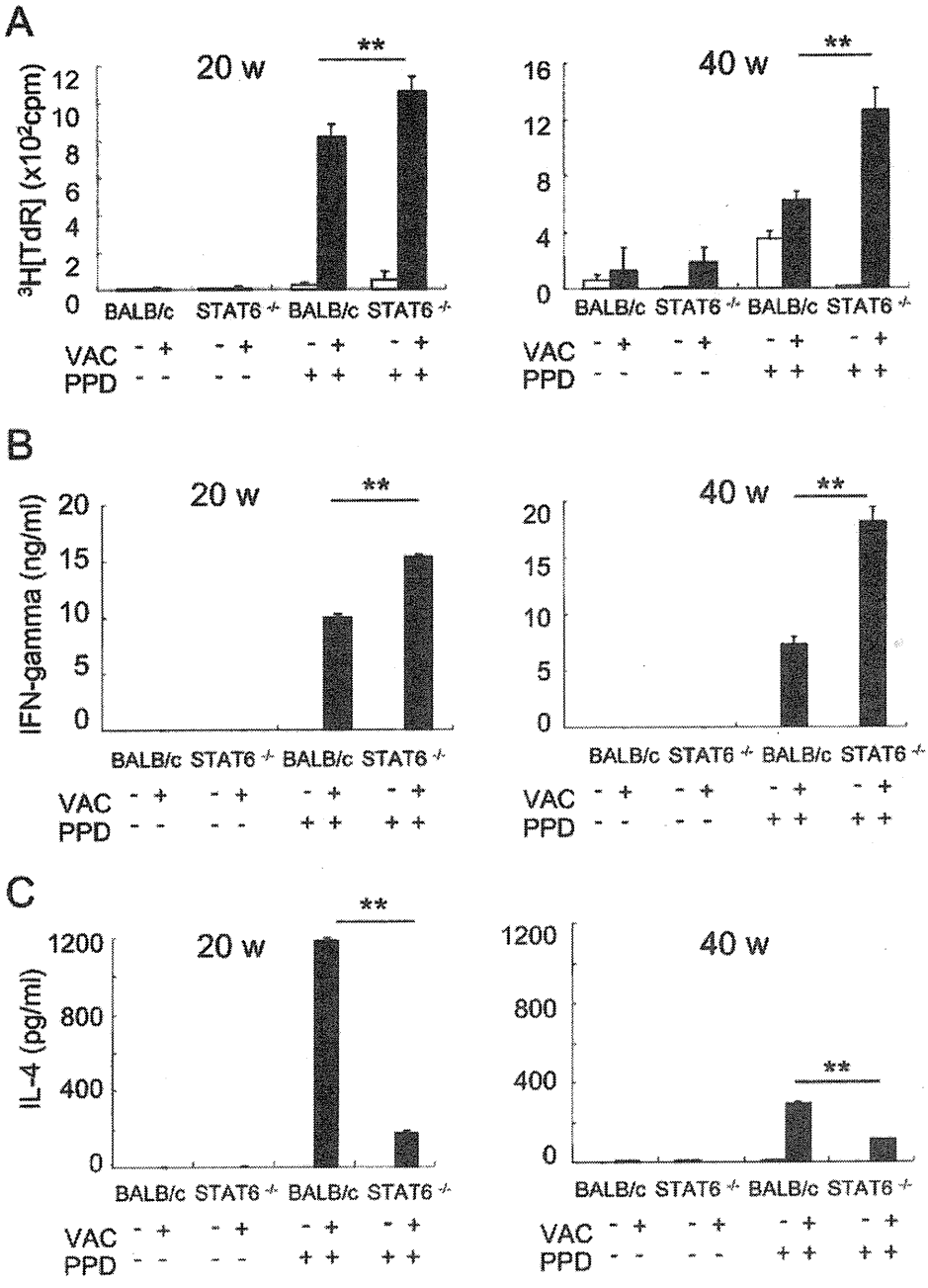

Fig. 6. Immune responses of lymph node cells derived from BALB/c and STAT6 knockout mice after stimulation with PPD. 2.5×10^6 lymph node cells were cultured with or without 10 μg/ml of PPD for 5 days. Uptake of ^{3}H labeled thymidine was determined (A). The amounts of IFN-gamma (B) and IL-4 (C) in the culture supernatants were determined by ELISA. Black columns, vaccinated BALB/c or STAT6 knockout mice. White columns, unvaccinated BALB/c and STAT6 knockout mice. $^{**}P < 0.01$ vaccinated BALB/c mice versus vaccinated STAT6 mice.

relatively TH1-prone than BALB/c mice [24], and resist equally against *M. tuberculosis* challenge [25,26].

In this study, the loss of protection was not dependent on the elimination of vaccinated BCG in the animals (Figs. 1 and 5) or advanced age of the mice (Fig. 4). Ito et al. reported that even 24-month old mice can be protected by BCG vaccination to a comparable level as young mice [27]. BCG also induced similar protection in old (60 month old) and middle aged guinea pigs as compared with young guinea pigs [28]. Thus BCG is likely to induce protection for a certain period of time after vaccination, but our study shows its efficacy is eventually lost over time following vaccination in mouse models.

The decline of BCG efficacy was reported in the human studies. One study enrolled 54,239 persons in England showed the efficacy of BCG within the first 5 years are 84% but it was gradually decreased to 59% after 15 years [8]. Another study performed in the United States enrolled 64,136 persons, also reported rapid loss of BCG efficacy 4 years after vaccination [9]. From these reports, it would be probably reasonable to consider that loss of protection occurred in BCG-vaccinated human with time. However one report showed that efficacy maintained over 50 years by the survey of relatively small (2792) number of subjects. Our finding prompts the requirement for the exact survey of the duration of effectiveness of BCG in adult human beings.

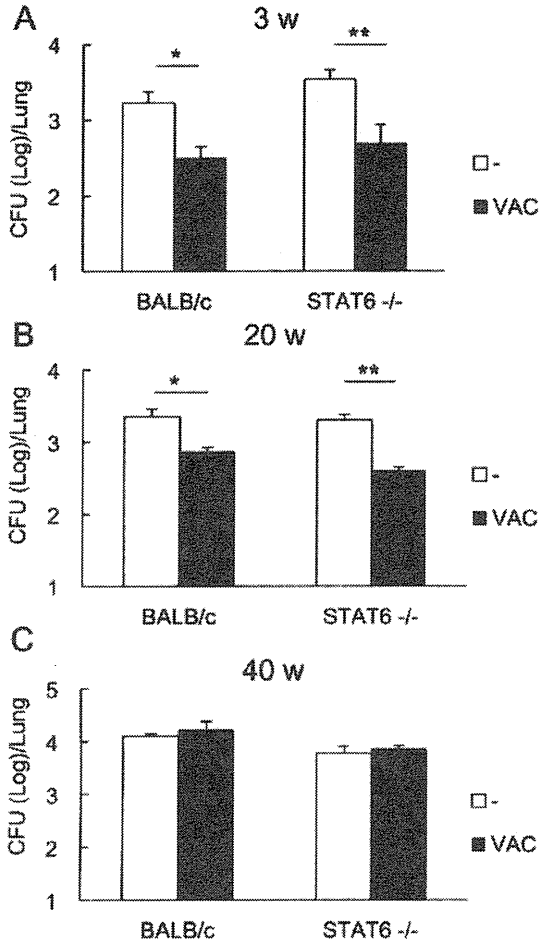

Fig. 7. Influence of time on BCG-induced protection in BALB/c and STAT6 knockout mice. Three, 20, and 40 weeks after BCG vaccination, BCG-vaccinated BALB/c and STAT6 knockout (black columns), unvaccinated BALB/c and STAT6 knockout mice (white columns) were challenged with 10^5–10^6 CFU of KM resistant BCG intratracheally. Five weeks later, mice were sacrificed and CFUs of KM resistant BCG in lungs were determined. $^{**}P < 0.01$; $^{*}P < 0.05$ versus unvaccinated mice.

If the mice model established in this study would reflect variable or low protectiveness of BCG vaccination against adult pulmonary tuberculosis, this model would be useful in the analysis of immune responses and evaluation of newly developed vaccines. Currently, prime-booster vaccination is one of the viable vaccination strategies [18]. This loss of BCG efficacy mouse model is useful for studying the regeneration of protectiveness after boosting with new vaccine candidates.

Sakai et al. recently reported a reduction in efficacy 12 weeks after BCG vaccination in mice [29]. They found a reduction in programmed cell death ligand 1 (PD-L1) expression on the antigen-expressing cell 3 weeks after BCG vaccination and programmed cell death 1 (PD-1) knockout mice acquired stronger protection following BCG vaccination. Because the PD-1-PD-L1 pathway negatively regulates antigen receptor signaling between T cells and APCs [30], they concluded that the PD-1-PD-L1 pathway-dependent impairment of TH1 immunity is involved in the reduction in BCG-induced protection. We also observed a reduction in TH1 immune responses to PPD in C57BL/6 mice (Fig. 3A) although this was still evident in BALB/c mice (Fig. 6B). In addition, analysis of BALB/c and STAT-6 knockout mice showed that the protectiveness of the BCG vaccination was lost despite the maintenance of TH1 immune responses to *M. tuberculosis* antigens (Figs. 6 and 7). Although activation of the PD-1-PD-L1 pathway participates in a reduction of TH1 immunity upon BCG vaccination [29], our results suggest that the reduction of TH1 immune responses does not fully explain the loss of BCG-induced protection.

Although responses of lymph node cells and splenic $CD4^+$ cells to *M. tuberculosis* antigens are different between C57BL/6 (Fig. 3) and BALB/c (Fig. 6) mice, both mice similarly lost protectiveness of BCG at 40 weeks post vaccination, implying that an unknown common mechanism caused loss of effectiveness in both mice. IFN-gamma plays a central role in acquired protective immunity against tuberculosis in both mice [11,13,31] and humans [14,15]. However solely detecting the production of IFN-gamma is not a sufficient biomarker to predict protective status from tuberculosis [32] and Scanga et al. reported reactivation of persistent tuberculosis despite continued expression of interferon gamma in mice [33]. Loss of protectiveness of the BCG vaccination in spite of maintenance of the IFN-gamma productivity of T cells following stimulation with PPD (Figs. 6 and 7) suggests that it might be due to unresponsiveness to IFN-gamma signaling or some unknown mechanism separated from IFN-gamma signaling. One possible mechanism is regulatory T cells (Tregs). However, Sakai et al. predicted a minor contribution of Tregs in the reduction of BCG-induced protectiveness [29] and we and other groups suggested minor roles for Tregs in mycobacteria infection [34–36], although others have reported the contribution of Tregs in immune suppression in mycobacterial infection [37,38]. In our preliminary experiments, robust IL-10 production was observed from lymph node cells and purified $CD4^+$ cells derived from mice after 40 weeks vaccination following PPD stimulation (our unpublished data). Since IL-10 is an immunosuppressive cytokine, it may be one of the possible factors involved in loss of BCG-induced protection. In order to clarify the mechanism of reduced protection and the possible roles of immunosuppressive cytokines and cells, mice that had received the BCG vaccination a long time ago should be used in future studies.

5. Conclusion

This study shows that a reduction in efficacy of the BCG vaccination against mycobacterial infection occurs in mice over time following vaccination. The duration from vaccination should be considered when assessing the variation of BCG efficacy against adult pulmonary tuberculosis. This mouse model demonstrating the loss of BCG effectiveness should be useful for understanding the BCG vaccine and aid the development effective tuberculosis vaccines.

Acknowledgments

This work was supported by grants from the Ministry of Education Culture Sports Science and Technology, Ministry of Health, Labour and Welfare (Research on Emerging and Re-emerging Infectious Diseases, Health Sciences Research Grants), The Japan Health Sciences Foundation (to Y.O., T.T., S.Y., K.K., and S. M.). We also thank Sara Matsumoto for assistance with the experiments and heartfelt encouragement.

References

[1] WHO. http://www.who.int/tb/publications/global_report/2009/update/en/index.html; 2010.
[2] WHO. BCG: bad news from India. Lancet 1980;1(8159):73–4.
[3] Fine PE. Variation in protection by BCG: implications of and for heterologous immunity. Lancet 1995;346(8986):1339–45.
[4] Colditz GA, Brewer TF, Berkey CS, Wilson ME, Burdick E, Fineberg HV, et al. Efficacy of BCG vaccine in the prevention of tuberculosis. Meta-analysis of the published literature. JAMA 1994;271(9):698–702.
[5] Behr MA, Wilson MA, Gill WP, Salamon H, Schoolnik GK, Rane S, et al. Comparative genomics of BCG vaccines by whole-genome DNA microarray. Science 1999;284(5419):1520–3.

[6] Brandt L, Feino Cunha J, Weinreich Olsen A, Chilima B, Hirsch P, Appelberg R, et al. Failure of the *Mycobacterium bovis* BCG vaccine: some species of environmental mycobacteria block multiplication of BCG and induction of protective immunity to tuberculosis. Infect Immun 2002;70(2):672–8.
[7] Clemens JD, Chuong JJ, Feinstein AR. The BCG controversy. A methodological and statistical reappraisal. JAMA 1983;249(17):2362–9.
[8] Comstock GW, Palmer CE. Long-term results of BCG vaccination in the southern United States. Am Rev Respir Dis 1966;93(February (2)):171–83.
[9] Hart PD, Sutherland I. BCG and vole bacillus vaccines in the prevention of tuberculosis in adolescence and early adult life. Br Med J 1977;2(July (6082)):293–5.
[10] Aronson NE, Santosham M, Comstock GW, Howard RS, Moulton LH, Rhoades ER, et al. Long-term efficacy of BCG vaccine in American Indians and Alaska Natives: a 60-year follow-up study. JAMA 2004;291(May (17)):2086–91.
[11] Kawamura I, Tsukada H, Yoshikawa H, Fujita M, Nomoto K, Mitsuyama M. IFN-gamma-producing ability as a possible marker for the protective T cells against *Mycobacterium bovis* BCG in mice. J Immunol 1992;148(9):2887–93.
[12] Cooper AM, Dalton DK, Stewart TA, Griffin JP, Russell DG, Orme IM. Disseminated tuberculosis in interferon gamma gene-disrupted mice. J Exp Med 1993;178(6):2243–7.
[13] Flynn JL, Chan J, Triebold KJ, Dalton DK, Stewart TA, Bloom BR. An essential role for interferon gamma in resistance to *Mycobacterium tuberculosis* infection. J Exp Med 1993;178(6):2249–54.
[14] Jouanguy E, Altare F, Lamhamedi S, Revy P, Emile JF, Newport M, et al. Interferon-gamma-receptor deficiency in an infant with fatal bacille Calmette-Guerin infection. N Engl J Med 1996;335(26):1956–61.
[15] Newport MJ, Huxley CM, Huston S, Hawrylowicz CM, Oostra BA, Williamson R, et al. A mutation in the interferon-gamma-receptor gene and susceptibility to mycobacterial infection. N Engl J Med 1996;335(26):1941–9.
[16] Orme IM. Induction of nonspecific acquired resistance and delayed-type hypersensitivity, but not specific acquired resistance in mice inoculated with killed mycobacterial vaccines. Infect Immun 1988;56(12):3310–2.
[17] Flynn JL, Chan J. Immunology of tuberculosis. Annu Rev Immunol 2001;19:93–129.
[18] Young DB, Perkins MD, Duncan K, Barry 3rd CE. Confronting the scientific obstacles to global control of tuberculosis. J Clin Invest 2008;118(4):1255–65.
[19] Kaplan MH, Schindler U, Smiley ST, Grusby MJ. Stat6 is required for mediating responses to IL-4 and for development of Th2 cells. Immunity 1996;4(3):313–9.
[20] Shimoda K, van Deursen J, Sangster MY, Sarawar SR, Carson RT, Tripp RA, et al. Lack of IL-4-induced Th2 response and IgE class switching in mice with disrupted Stat6 gene. Nature 1996;380(6575):630–3.
[21] Takeda K, Tanaka T, Shi W, Matsumoto M, Minami M, Kashiwamura S, et al. Essential role of Stat6 in IL-4 signalling. Nature 1996;380(6575):627–30.
[22] Heinzel FP, Sadick MD, Holaday BJ, Coffman RL, Locksley RM. Reciprocal expression of interferon gamma or interleukin 4 during the resolution or progression of murine leishmaniasis. Evidence for expansion of distinct helper T cell subsets. J Exp Med 1989;169(January (1)):59–72.
[23] Bohn E, Heesemann J, Ehlers S, Autenrieth IB. Early gamma interferon mRNA expression is associated with resistance of mice against *Yersinia enterocolitica*. Infect Immun 1994;62(July (7)):3027–32.
[24] Wakeham J, Wang J, Xing Z. Genetically determined disparate innate and adaptive cell-mediated immune responses to pulmonary *Mycobacterium bovis* BCG infection in C57BL/6 and BALB/c mice. Infect Immun 2000 Dec;68(12):6946–53.
[25] Chackerian AA, Behar SM. Susceptibility to *Mycobacterium tuberculosis*: lessons from inbred strains of mice. Tuberculosis (Edinb) 2003;83(5):279–85.
[26] Jung YJ, Ryan L, LaCourse R, North RJ. Differences in the ability to generate type 1T helper cells need not determine differences in the ability to resist *Mycobacterium tuberculosis* infection among mouse strains. J Infect Dis 2009;199(June (12)):1790–6.
[27] Ito T, Takii T, Maruyama M, Hayashi D, Wako T, Asai A, et al. Effectiveness of BCG vaccination to aged mice. Immun Ageing 2010;7:12.
[28] Komine-Aizawa S, Yamazaki T, Yamazaki T, Hattori S, Miyamoto Y, Yamamoto N, et al. Influence of advanced age on *Mycobacterium bovis* BCG vaccination in guinea pigs aerogenically infected with *Mycobacterium tuberculosis*. Clin Vaccine Immunol 2010;17(10):1500–6.
[29] Sakai S, Kawamura I, Okazaki T, Tsuchiya K, Uchiyama R, Mitsuyama M. PD-1-PD-L1 pathway impairs T(h)1 immune response in the late stage of infection with *Mycobacterium bovis* bacillus Calmette-Guerin. Int Immunol 2010;22(12):915–25.
[30] Okazaki T, Honjo T. PD-1 and PD-1 ligands: from discovery to clinical application. Int Immunol 2007;19(7):813–24.
[31] Orme IM, Roberts AD, Griffin JP, Abrams JS. Cytokine secretion by CD4 T lymphocytes acquired in response to *Mycobacterium tuberculosis* infection. J Immunol 1993;151(1):518–25.
[32] Parida SK, Kaufmann SH. The quest for biomarkers in tuberculosis. Drug Discov Today 2010;15(3–4):148–57.
[33] Scanga CA, Mohan VP, Yu K, Joseph H, Tanaka K, Chan J, et al. Depletion of CD4(+) T cells causes reactivation of murine persistent tuberculosis despite continued expression of interferon gamma and nitric oxide synthase 2. J Exp Med 2000;192(3):347–58.
[34] Ozeki Y, Sugawara I, Udagawa T, Aoki T, Osada-Oka M, Tateishi Y, et al. Transient role of CD4+CD25+ regulatory T cells in mycobacterial infection in mice. Int Immunol 2010;22(3):179–89.
[35] Quinn KM, McHugh RS, Rich FJ, Goldsack LM, de Lisle GW, Buddle BM, et al. Inactivation of CD4+ CD25+ regulatory T cells during early mycobacterial infection increases cytokine production but does not affect pathogen load. Immunol Cell Biol 2006;84(5):467–74.
[36] Quinn KM, Rich FJ, Goldsack LM, de Lisle GW, Buddle BM, Delahunt B, et al. Accelerating the secondary immune response by inactivating CD4(+)CD25(+) T regulatory cells prior to BCG vaccination does not enhance protection against tuberculosis. Eur J Immunol 2008;38(3):695–705.
[37] Kursar M, Koch M, Mittrucker HW, Nouailles G, Bonhagen K, Kamradt T, et al. Cutting edge: regulatory T cells prevent efficient clearance of *Mycobacterium tuberculosis*. J Immunol 2007;178(5):2661–5.
[38] Scott-Browne JP, Shafiani S, Tucker-Heard G, Ishida-Tsubota K, Fontenot JD, Rudensky AY, et al. Expansion and function of Foxp3-expressing T regulatory cells during tuberculosis. J Exp Med 2007;204(9):2159–69.

European Journal of Immunology SHORT COMMUNICATION

IL-17 production by γδ T cells is important for the antitumor effect of *Mycobacterium bovis* bacillus Calmette-Guérin treatment against bladder cancer

Ario Takeuchi[1,2], Takashi Dejima[1,2], Hisakata Yamada[1], Kensuke Shibata[1], Risa Nakamura[1], Masatoshi Eto[3], Tatsuya Nakatani[4], Seiji Naito[2] and Yasunobu Yoshikai[1]

[1] Division of Host Defense, Medical Institute of Bioregulation, Kyushu University, Fukuoka, Japan
[2] Department of Urology, Graduate School of Medical Science, Kyushu University, Fukuoka, Japan
[3] Department of Urology, Graduate School of Medical Sciences, Kumamoto University, Kumamoto, Japan
[4] Department of Urology, Osaka City University Graduate School of Medicine, Osaka, Japan

Intravesical inoculation of *Mycobacterium bovis* bacillus Calmette-Guérin (BCG) has been used for the treatment of bladder cancer. Recent studies implied the requirement of neutrophil infiltration for the antitumor effect. In this study, we found that IL-17 was produced in the bladder after BCG treatment, preceding the infiltration of neutrophils. Neutrophils in the bladder after BCG treatment were reduced in IL-17-deficient mice, in which BCG-induced antitumor effect against intravesically inoculated bladder cancer was abolished. Notably, the level of IL-17 production and the number of neutrophils in BCG-treated bladder was reduced in γδ T-cell-deficient mice but not in CD4-depleted mice. Survival of bladder cancer-inoculated γδ T-cell-deficient mice was not improved by BCG treatment. These results suggest that IL-17-producing γδ T cells play a key role in the BCG-induced recruitment of neutrophils to the bladder, which is essential for the antitumor activity against bladder cancer.

Key words: γδ T cells · Bladder tumor · BCG · IL-17 · Neutrophils

Supporting Information available online

Introduction

In 1976, Morales *et al.* reported intravesical inoculation of *Mycobacterium bovis* BCG as an effective adjuvant therapy for bladder cancers [1]. Thereafter, intravesical immunotherapy with BCG has been used for 30 years, however the antitumor effector mechanisms remain elusive. Recent studies demonstrated that neutrophils infiltrated in the bladder after BCG treatment played a key role in the antitumor effect [2]. Expression of TRAIL on neutrophils in voided urine following BCG therapy suggests a direct antitumor effect of neutrophils [3, 4]. In addition, neutrophils isolated from BCG-treated bladder produced CC (*e.g.* MIP-1α) as well as CXC chemokines (*e.g.* IL-8 and GRO-α). The chemokines released by activated neutrophils attract monocytes, which in turn result in BCG-induced CD4 T-cell-migration [2]. Th1-polarized cell-mediated immunity, which includes NK cells, and $CD8^+$ and $CD4^+$ T cells, was also involved in the antitumor effect of BCG immunotherapy [5–7]. Thus, neutrophils

Correspondence: Dr. Hisakata Yamada
e-mail: hisakata@bioreg.kyushu-u.ac.jp

might exert antitumor effect directly and indirectly. However, at present, the mechanism of neutrophil infiltration after BCG treatment is not fully understood.

IL-17 (also known as IL-17A) is a T-cell-derived proinflammatory cytokine, which is involved in various pathogenesis where neutrophils are involved. IL-17 induces mobilization of neutrophils indirectly *via* production of several cytokines, growth factors, and CXC chemokines [8]. IL-17 is produced by a recently identified subset of helper $CD4^+$ T cells, Th17 cells, which contribute to various inflammatory disorder as well as host defense [9]. However, increasing evidence revealed that another subset of T cells, namely γδ T cells, could even play a dominant role as the source of IL-17 *in vivo*. We found that γδ T cells in the peritoneal cavity produced IL-17 immediately after *Escherichia coli* infection, which is critical to the infiltration of neutrophils [10]. Furthermore, it was reported that IL-17 production in pulmonary infection with BCG was mediated by γδ T cells [11]. In the present study, we found BCG treatment in murine bladder also induced IL-17 production by γδ T cells, which play essential role in local neutrophil infiltration and antitumor effect against bladder cancer.

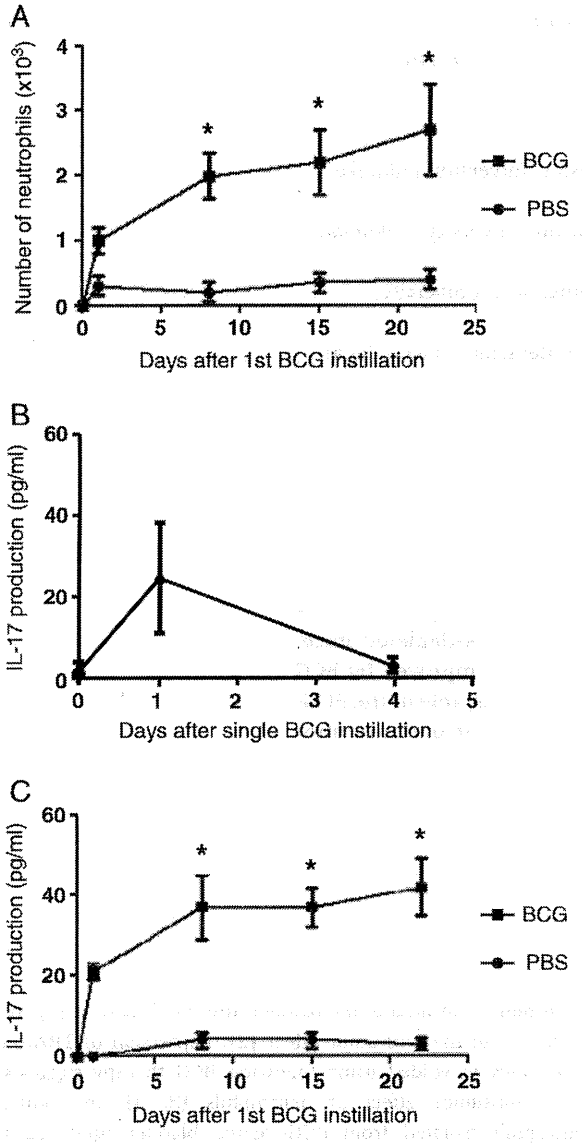

Figure 1. Intravesical neutrophil infiltration and IL-17 production after BCG treatment. B6 mice were intravesically injected with BCG or PBS on days 0, 7, 14, and 21. On days 0, 1, 8, 15, and 22, the number of neutrophils (A) and the level of IL-17 production (C) in the bladder were analyzed. Each group consisted of five mice. (B) Kinetics of the level of IL-17 production after single injection of BCG in the bladder ($n = 3$). Representative data of three separate experiments are shown. *$p<0.05$, Student's t-test.

Results and discussion

Vesical neutrophil infiltration after BCG treatment is mediated by IL-17

Recent studies demonstrated that neutrophils infiltrated in the bladder after BCG treatment played a key role in the antitumor effect [2]. In this study, we first examined the kinetics of neutrophil infiltration induced by weekly treatment with BCG. Significant infiltration of neutrophils was observed from one wk

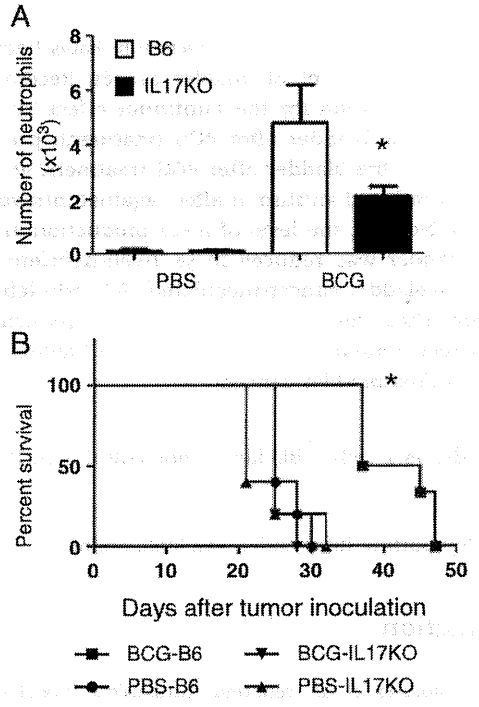

Figure 2. Involvement of IL-17 in the neutrophil infiltration and antitumor effect of BCG treatment. (A) B6 and IL-17KO mice were intravesically injected with BCG or PBS on days 0, 7, 14, and 21. On day 22, the number of neutrophils in the bladder was analyzed. Each group consisted of five mice. *$p<0.05$, Student's t-test. (B) B6 and IL-17KO mice were intravesically inoculated with 1×10^5 MB49 tumor cells on day 0 and received weekly intravesical injections of BCG or PBS from day 1 to 22. Each group consisted of five mice. Representative data of three separate experiments are shown. *$p<0.05$ compared with other three groups, log-rank test.

after starting BCG treatment, and it gradually increased during the observation period (Fig. 1A). We then examined intravesical IL-17 production after single BCG administration. As shown in Fig. 1B, IL-17 production was induced as early as 1 day after BCG injection, but lasted less than 5 days. During the course of repeated BCG administration, similar level of IL-17 production was induced after each injection (Fig. 1C). In order to determine the importance of IL-17 in the infiltration of neutrophils after BCG treatment, we examined the number of intravesical neutrophils in IL-17-deficient mice 22 day after starting BCG treatment. Infiltration of neutrophils was significantly reduced in IL-17-deficient mice (Fig. 2A). Therefore, IL-17 was involved in the infiltration of neutrophils into the bladder after BCG treatment.

Requirement for IL-17 in the antitumor effects of intravesical BCG treatment

To examine the significance of IL-17-induced neutrophil infiltration in the antitumor effect of BCG therapy, IL-17 KO mice were inoculated with MB49 bladder cancer cells before BCG treatment (Fig. 2B). The control B6 mice treated with BCG exhibited significantly longer survival compared to PBS-treated mice. On the other hand, there was no difference in the survival between BCG- and PBS-treated IL-17-deficient mice. There was also no difference in the survival of PBS-treated B6 and IL-17-deficient mice. We confirmed that depletion of neutrophils completely abrogated the antitumor effect of BCG therapy (data not shown), as was previously demonstrated by others [2]. Thus, it was revealed that IL-17-induced neutrophil infiltration was essential for the antitumor effect of intravesical treatment of BCG.

In contrast to our results, there have been reports implicating IL-17 with tumor progression. By acting on stromal cells and fibroblasts, IL-17 induces angiogenesis factors, which enhances tumor growth [12, 13]. It is possible that the antitumor effect of neutrophil infiltration overwhelmed the tumor-promoting effect of IL-17 in the case of bladder tumor. Alternative explanation for the discrepancy was the short duration of IL-17 production after each injection of BCG, which might not be enough for the tumor-promoting effect (Fig. 1B). In addition, there are reports showing

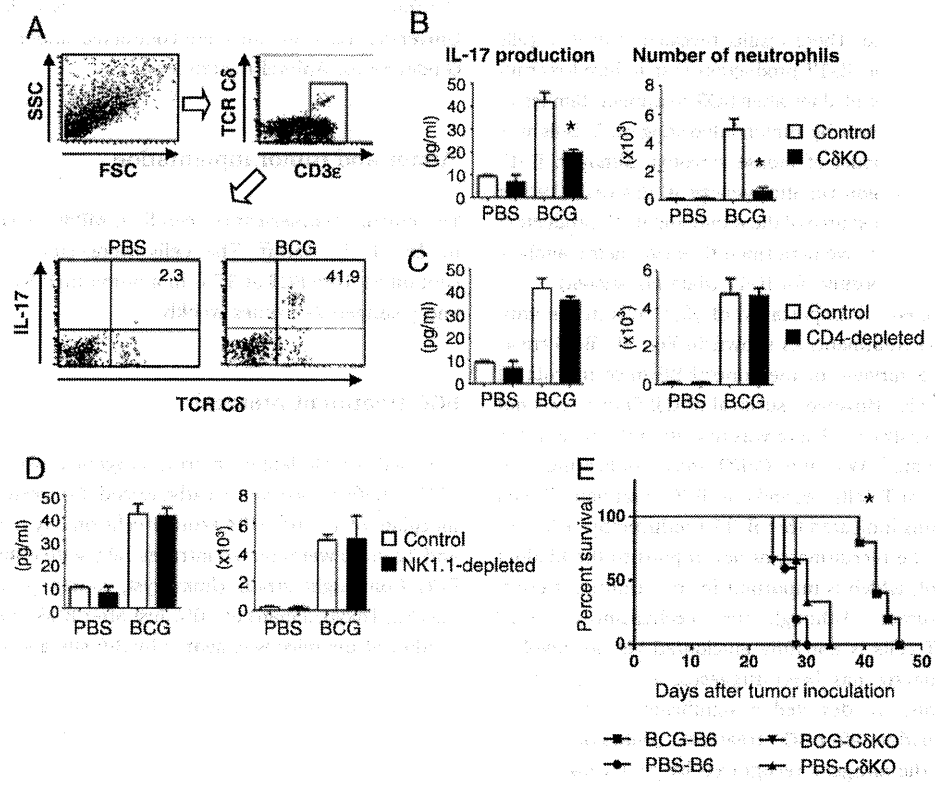

Figure 3. Importance of γδ T cells in IL-17 production, neutrophil infiltration, and the antitumor effect of BCG treatment. (A) Flow cytometric analysis of IL-17 production by the lymphocytes in the bladder of PBS (left)- or BCG (right)-treated mice was performed after brief in vitro culture without stimulation. Representative dot plots of IL-17 and TCR Cδ expression are shown after gating on $CD3^+$ lymphocytes. The number in upper right quadrant indicates the percent of $IL\text{-}17^+$ cells in TCR $Cδ^+$ cells. (B) B6 (control) and CδKO mice were intravesically injected with BCG or PBS on days 0, 7, 14, and 21. A group of PBS (control) or BCG-treated B6 mice received repeated i.p. injection of anti-CD4 mAb (C), anti-NK1.1 mAb (D), or the respective isotype control mAbs on days −1, 6, 13, and 20. Depletion of the target cell populations after mAb administration was confirmed by flow cytometry (Supporting Information Fig. 1). The level of IL-17 production (left) and the number of neutrophils (right) were measured on day 22. Each group consisted of five mice. Representative data of three separate experiments are shown. *$p<0.05$, Student's t-test. (E) B6 and CδKO mice were intravesically inoculated with 1×10^5 MB49 tumor cells on day 0 and were received weekly intravesical injection with BCG or PBS from day 1 to 22. Each group consisted of five mice. Representative data of two separate experiments are shown. *$p<0.05$ compared with other three groups, log-rank test.

tumor-inhibitory effects of IL-17 [14–17]. Further investigation is necessary to identify factors that dictate anti- *versus* pro-tumor effects of IL-17 [18].

γδ T cells are the major source of IL-17 production after BCG treatment

In order to identify the cell subset(s) responsible for the IL-17 production after BCG treatment, we harvested mononuclear cells in the bladder of BCG- or PBS-treated mice at day 22 and performed flow cytometric analysis of *ex vivo* intracellular staining for IL-17. We detected $CD3^+$ cells producing IL-17 in BCG-treated bladder, and the IL-17^+ cells were mostly TCR $\gamma\delta^+$ (Fig. 3A). To directly address which cell population is important as the source of IL-17, we measured IL-17 production and neutrophil infiltration in the bladder of γδ T-cell-deficient mice (CδKO), and CD4 or NK1.1-depleted mice (Fig. 3B and D). We found that BCG-treated CδKO mice showed significant reduction of IL-17 production and neutrophil infiltration compared with BCG-treated control mice. On the other hand, there was no difference in either IL-17 production or neutrophil count between CD4 or NK cell-depleted mice and the control mice. These results revealed that γδ T cells significantly contributed to IL-17 production that induced recruitment of neutrophlis to the bladder after BCG treatment. Similar to our results, IL-17 production by tumor infiltrating γδ T cells was recently reported in a model of mouse sarcoma, although IL-17 supported tumor progression *via* angiogenesis in this case [19]. In order to define the cellular source of the remaining IL-17 production in BCG-treated CδKO mice, we performed flow cytometric analysis but failed to detect cells positive for IL-17 (data not shown).

We lastly examined the importance of γδ T cells in the antitumor effect of BCG treatment. As shown in Fig. 3E, BCG treatment prolonged the survival of the control B6 mice inoculated with MB49 tumor cells. However, survival of CδKO mice was not improved by BCG treatment. There was also no difference in the survival of PBS-treated WT and CδKO mice, indicating that antitumor effect of γδ T cells depends on BCG treatment. Taken together, these results indicated that IL-17 produced by γδ T cells plays a key role in the recruitment of neutrophlis to the bladder after BCG treatment, which is important for the antitumor effect against bladder tumor. Although the mechanism of IL-17 production by γδ T cells is not fully elucidated yet, an involvement of IL-23-signaling has been suggested [10, 11, 20]. In agreement with this, we detected a significant level of IL-23 production in the bladder after BCG treatment (data not shown). However, because the antigens recognized by γδ T cells remain unclear, possible involvement of antigenic stimulation on BCG-induced IL-17 production by γδ T cells is not excluded.

Concluding remarks

We found in this study that γδ T cells were involved in the antitumor effect of intravesical BCG treatment *via* IL-17 production. Interestingly, Yuasa *et al.* reported that intravesical administration of γδ T cells exerted antitumor activity against bladder tumor, which is thought to be mediated by the direct cytotoxic activity to the tumor cells [21]. Importantly, human γδ T cells are also known for their antitumor effect [22]. Because γδ T cells exert effector function in an MHC-unrestricted manner, these findings suggest that γδ T cells could be a good target of universally applicable immunotherapy against bladder cancer.

Materials and methods

Mice

C57BL/6 (B6) mice were purchased from Japan SLC (Hamamatsu, Japan). CδKO and IL-17KO mice (B6 background) were kindly provided by Dr. S. Itohara and Dr. Y. Iwakura, respectively. The mice were bred in specific pathogen-free conditions in our institute. 6- to 8-wk-old female mice were used for the experiments. This study was approved by the Committee of Ethics on Animal Experiment in Faculty of Medicine, Kyushu University. Experiments were conducted under the control of the Guideline for Animal Experiment.

Tumor and tumor inplantation

The murine bladder cancer cell line, MB49, was kindly provided by Dr. T. L. Ratliff. The cells were cultured in RPMI-1640 containing 10% FCS at 37°C in a humidified 5% CO_2 atmosphere and passaged 2–3 times weekly.

BCG treatment protocol

We used a well-defined murine syngeneic bladder tumor model [23]. Briefly, mice were catheterized to receive an intravesical inoculate of 1×10^5 MB49 tumor cells on day 0. On days 1, 8, 15, and 22, mice were treated intravesically with either 3×10^6 CFU of BCG Connaught strain (Immucyst, kindly provided by Nippon kayaku, Tokyo, Japan) or PBS. Just after BCG or PBS injection, the urethra of the mice was ligated by 3-0 silk and released 3 h later.

Isolation of neutrophils and lymphocytes for flow cytometric analysis

To harvest neutrophils and lymphocytes, the bladder was minced to yield 1–2 mm pieces and were incubated in a mixture of 1 mg/mL collagenase (Invitrogen, Carlsbad, CA, USA) and 20 μg/mL DNase (Sigma-Aldrich, St. Louis, MO, USA) in RPMI 1640 containing 10% FCS for 90 min at 37°C. The following antibodies were used for flow cytometric analysis: FITC-conjugated anti-Gr-1 (RB6-8C5), anti-TCR Cδ (GL3), and anti-CD4 (RM4-5)

mAbs, PE-conjugated anti-I-A/E (M5/114.15.2), anti-NK1.1 (PK136), anti-CD8 (53-6.7) mAbs, allophycocyanin-conjugated anti-CD3e (145-2C11) mAb (BD Biosciences, San Diego, CA, USA), and PE-conjugated donkey anti-mouse IgG polyclonal antibody (eBioscience, San Diego, CA, USA). Stained cells were run on a FACS Calibur flow cytometer (BD Biosciences) after adding propidium iodide (1 μg/mL) in order to exclude the dead cells. The data were analyzed using Cell Quest software (BD Biosciences).

Intracellular cytokine staining

Freshly isolated lymphocytes from the bladder were immediately incubated with 10 μg/mL befeldin A (Sigma-Aldrich) in RPMI containing 10% FCS at 37°C for 6 h. Cells were first stained with mAbs for surface molecules and were then fixed and permeabilized using BD Perm/Wash solution (BD Biosciences) and stained with PE-conjugated anti-mIL-17 (TC11-18H10.1) mAb (BD Biosciences).

In vivo depletion of neutrophils, $CD4^+$ cells, and $NK1.1^+$ cells

Two hundred micrograms of anti-Gr-1 mAb (RB6-8C5), anti-CD4 mAb (GK1.5), or anti-NK mAb (PK136) or the isotype control mAb was given i.p. every 7 days. Depletion of each cell subset was confirmed by flow cytometric analysis.

ELISA for measurement of IL-17 production

Bladders were dissected from BCG-treated or PBS-treated mice and minced in 200 μL of PBS. After a centrifugation, IL-17 in the supernatant was measured by mouse IL-17 DuoSet ELISA Development System (R&D Systems, Minneapolis, MN, USA), according to the manufacturer's instructions.

Statistical analyses

Survival of mice was evaluated using Kaplan–Meier plots and the log-rank test. Difference in the amounts of IL-17 production or neutrophil counts were analyzed by Student's *t*-test using GraphPad Prism 5.0 software (Prism Graphpad, San Diego, CA, USA). Differences with p values of <0.05 were considered statistically significant.

Acknowledgements: This work was supported in part by a Grant-in-Aid for Scientific Research from the Japan Society for Promotion of Science (H. Y. and Y. Y.), and by the program of Founding Research Centers for Emerging and Reemerging Infectious Diseases launched as a project commissioned by the Ministry of Education, Culture, Sports, Science and Technology (MEXT), Japan (Y. Y.).

Conflict of interest: The authors declare no financial or commercial conflict of interest.

References

1 Morales, A., Eidinger, D. and Bruce, A. W., Intracavitary bacillus Calmette-Guérin in the treatment of superficial bladder tumors. *J. Urol.* 1976. **116**: 180–183.

2 Suttmann, H., Riemensberger, J., Bentien, G., Schmaltz, D., Stockle, M., Jocham, D., Bohle, A. and Brandau, S., Neutrophil granulocytes are required for effective bacillus Calmette-Guérin immunotherapy of bladder cancer and orchestrate local immune responses. *Cancer Res.* 2006. **66**: 8250–8257.

3 Ludwig, A. T., Moore, J. M., Luo, Y., Chen, X., Saltsgaver, N. A., O'Donnell, M. A. and Griffith, T. S., Tumor necrosis factor-related apoptosis-inducing ligand: a novel mechanism for bacillus Calmette-Guérin-induced antitumor activity. *Cancer Res.* 2004. **64**: 3386–3390.

4 Kemp, T. J., Ludwig, A. T., Earel, J. K., Moore, J. M., Vanoosten, R. L., Moses, B., Leidal, K. *et al.*, Neutrophil stimulation with *Mycobacterium bovis* bacillus Calmette-Guérin (BCG) results in the release of functional soluble TRAIL/Apo-2L. *Blood* 2005. **106**: 3474–3482.

5 Brandau, S., Suttmann, H., Riemensberger, J., Seitzer, U., Arnold, J., Durek, C., Jocham, D. *et al.*, Perforin-mediated lysis of tumor cells by *Mycobacterium bovis* bacillus Calmette-Guérin -activated killer cells. *Clin. Cancer Res.* 2000. **6**: 3729–3738.

6 Brandau, S., Riemensberger, J., Jacobsen, M., Kemp, D., Zhao, W., Zhao, X., Jocham, D. *et al.*, NK cells are essential for effective BCG immunotherapy. *Int. J. Cancer* 2001. **92**: 697–702.

7 Ratliff, T. L., Ritchey, J. K., Yuan, J. J., Andriole, G. L. and Catalona, W. J., T-cell subsets required for intravesical BCG immunotherapy for bladder cancer. *J. Urol.* 1993. **150**: 1018–1023.

8 Kolls, J. K., Lindén, A., Interleukin-17 family members and inflammation. *Immunity* 2004. **21**: 467–476.

9 Korn, T., Bettelli, E., Oukka, M. and Kuchroo, V. K., IL-17 and Th17 Cells. *Annu. Rev. Immunol.* 2009. **27**: 485–517.

10 Shibata, K., Yamada, H., Hara, H., Kishihara, K. and Yoshikai, Y., Resident Vdelta1+gammadelta T cells control early infiltration of neutrophils after *Escherichia coli* infection *via* IL-17 production. *J. Immunol.* 2007, **178**: 4466–4472.

11 Umemura, M., Yahagi, A., Hamada, S., Begum, M. D., Watanabe, H., Kawakami, K., Suda, T. *et al.*, IL-17-mediated regulation of innate and acquired immune response against pulmonary *Mycobacterium bovis* bacille Calmette-Guérin infection. *J. Immunol.* 2007. **178**: 3786–3796.

12 Takahashi, H., Numasaki, M., Lotze, M. T. and Sasaki, H., Interleukin-17 enhances bFGF-, HGF- and VEGF-induced growth of vascular endothelial cells. *Immunol. Lett.* 2005. **98**: 189–193.

13 Numasaki, M., Fukushi, J., Ono, M., Narula, S. K., Zavodny, P. J., Kudo, T., Robbins, P. D. *et al.*, Interleukin-17 promotes angiogenesis and tumor growth. *Blood* 2003. **101**: 2620–2627.

14 Benchetrit, F., Ciree, A., Vives, V., Warnier, G., Gey, A., Sautes-Fridman, C., Fossiez, F. *et al.*, Interleukin-17 inhibits tumor cell growth by means of a T-cell-dependent mechanism. *Blood* 2002. **99**: 2114–2121.

15 Kryczek, I., Wei, S., Szeliga, W., Vatan, L. and Zou, W., Endogenous IL-17 contributes to reduced tumor growth and metastasis. *Blood* 2009. 114: 357–359.

16 Hirahara, N., Nio, Y., Sasaki, S., Minari, Y., Takamura, M., Iguchi, C., Dong, M. *et al.*, Inoculation of human interleukin-17 gene-transfected Meth-A fibrosarcoma cells induces T-cell-dependent tumor-specific immunity in mice. *Oncology* 2001. 61: 79–89.

17 Muranski, P., Boni, A., Antony, P. A., Cassard, L., Irvine, K. R., Kaiser, A., Paulos, C. M. *et al.*, Tumor-specific Th17-polarized cells eradicate large established melanoma. *Blood* 2008. 112: 362–373.

18 Silva-Santos, B., Promoting angiogenesis within the tumor microenvironment: the secret life of murine lymphoid IL-17-producing gammadelta T cells. *Eur. J. Immunol.* 2010. 40: 1873–1876.

19 Wakita, D., Sumida, K., Iwakura, Y., Nishikawa, H., Ohkuri, T., Chamoto, K., Kitamura, H., Nishimura, T., Tumor-infiltrating IL-17-producing gammadelta T cells support the progression of tumor by promoting angiogenesis. *Eur. J. Immunol.* 2010. 40: 1927–1937.

20 Sutton, C. E., Lalor, S. J., Sweeney, C. M., Brereton, C. F., Lavelle, E. C. and Mills, K. H., Interleukin-1 and IL-23 induce innate IL-17 production from gammadelta T cells, amplifying Th17 responses and autoimmunity. *Immunity* 2009. 31: 331–341.

21 Yuasa, T., Sato, K., Ashihara, E., Takeuchi, M., Maita, S., Tsuchiya, N., Habuchi, T. *et al.*, Intravesical administration of gammadelta T cells successfully prevents the growth of bladder cancer in the murine model. *Cancer Immunol. Immunother.* 2009. 58: 493–502.

22 Kabelitz, D., Wesch, D. and He, W., Perspectives of gammadelta T cells in tumor immunology. *Cancer Res.* 2007. 67: 5–8.

23 Gunther, J. H., Jurczok, A., Wulf, T., Brandau, S., Deinert, I., Jocham, D. and Bohle, A., Optimizing syngeneic orthotopic murine bladder cancer (MB49). *Cancer Res.* 1999. 59: 2834–2837.

Abbreviation: **GδKO:** γδ T-cell-deficient

Full correspondence: Dr. Hisakata Yamada, Division of Host Defense, Medical Institute of Bioregulation, Kyushu University, 3-1-1 Maidashi, Higashi-ku, Fukuoka 812-8582, Japan
Fax: +81-92-642-6973
e-mail: hisakata@bioreg.kyushu-u.ac.jp

Received: 23/6/2010
Revised: 15/10/2010
Accepted: 25/10/2010

Notch-Hes1 pathway is required for the development of IL-17–producing γδ T cells

Kensuke Shibata,[1] Hisakata Yamada,[1] Tetsuya Sato,[2] Takashi Dejima,[1] Masataka Nakamura,[1] Tomokatsu Ikawa,[3] Hiromitsu Hara,[4] Sho Yamasaki,[5] Ryoichiro Kageyama,[6] Yoichiro Iwakura,[7] Hiroshi Kawamoto,[3] Hiroyuki Toh,[2] and Yasunobu Yoshikai[1]

Divisions of [1]Host Defense and [2]Bioinformatics, Medical Institute of Bioregulation, Kyushu University, Fukuoka, Japan; [3] Laboratory for Lymphocyte Development, RIKEN Research Center for Allergy and Immunology, Yokohama, Japan; [4]Department of Biomolecular Sciences, Faculty of Medicine, Saga University, Saga, Japan; [5]Division of Molecular Immunology, Medical Institute of Bioregulation, Kyushu University, Fukuoka, Japan; [6]Division of Growth Regulation, Institute for Virus Research, Kyoto University, Kyoto, Japan; and [7]Division of Cell Biology, Center for Experimental Medicine, Institute of Medical Science, Tokyo University, Tokyo, Japan

Unlike conventional T cells, which are exported from the thymus as naive cells and acquire effector functions upon antigen encounter in the periphery, a subset of γδ T cells differentiates into effectors that produce IL-17 within the fetal thymus. We demonstrate here that intrathymic development of the naturally occurring IL-17–producing γδ T cells is independent of STAT3 and partly dependent on RORγt. Comparative gene-expression analysis identified Hes1, one of the basic helix-loop-helix proteins involved in Notch signaling, as a factor specifically expressed in IL-17–producing γδ T cells. Hes1 is critically involved in the development of IL-17–producing γδ T cells, as evidenced by their severe decrease in the thymi of *Hes1*-deficient fetal mice. Delta-like 4 (Dll4)–expressing stromal cells support the development of IL-17–producing γδ T cells in vitro. In addition, conditional Hes1 ablation in peripheral γδ T cells decreases their IL-17 production but not their IFN-γ production. These results reveal a unique differentiation pathway of IL-17–producing γδ T cells. (*Blood*. 2011;118(3):586-593)

Introduction

Conventional TCR αβ cells are exported from the thymus as naive T cells. After activation by exposure to their cognate antigens in the periphery, naive CD4$^+$ αβ T cells differentiate into different helper T-cell lineages such as Th1, Th2, and Th17 cells, depending on the cytokine milieu, which induce different combinations of transcription factors. STAT3, RORγt, and RORα, which are induced by combined signals from TGFβ and IL-6 receptors, play important roles in the differentiation of Th17 cells by binding to the promoter or the enhancer region of the *IL17* gene.[1-3] STAT3 also inhibits the expression of Foxp3, which suppresses the functions of RORγt.[4]

In addition to Th17 cells, several subsets of T cells produce IL-17. These include T cells lacking CD4 and CD8, CD8$^+$ T cells, invariant natural killer T cells (NKT cells), and TCR γδ T cells.[5-8] There is accumulating evidence that TCR γδ T cells could be the major source of IL-17 in various murine models of infection such as *Mycobacterium tuberculosis*, *Escherichia coli*, and *Listeria monocytogenes*.[9] IL-17–producing γδ T cells are also involved in the pathogenesis of autoimmune diseases such as experimental allergic encephalomyelitis, collagen-induced arthritis, chronic granulomatous disease, and ischemic brain injury.[10] Interestingly, even freshly isolated γδ T cells from the thymus produce IL-17 in response to phorbol myristate acetate (PMA) and ionomycin stimulation, indicating the functional differentiation within the thymus.[11] Such naturally occurring IL-17–producing γδ T cells were already detected at the fetal stage as early as on embryonic day 15 (E15), when γδ T cells began to develop.[11] Therefore, in γδ T cells, the development and functional differentiation to IL-17 producers coincidentally occur within the fetal thymus. Intrathymic functional differentiation has been well documented for NKT cells.[12] During intrathymic development, NKT cell precursors acquire either an IL-4– or an IFN-γ–producing function at different stages.[13] Furthermore, there is a population of NKT cells that differentiates into IL-17–producing cells in the thymus independently of IL-6 and STAT3.[6,14] Nevertheless, like Th17 cells, IL-17–producing NKT cells require RORγt for their development.[15] At present, the molecular mechanisms for the development of IL-17–producing γδ T cells have not been defined, although it has been shown that IL-17–producing γδ T cells developed normally in *IL-6*–deficient mice but were decreased in the absence of TGF-β1.[16,17]

In the present study, we found that Hes1, one of the basic helix-loop-helix (bHLH) proteins induced by Notch signaling, was specifically expressed in IL-17–producing γδ T cells. Furthermore, Hes1, rather than STAT3 and RORγt, was critically involved in intrathymic development of IL-17–producing γδ T cells. Expression of *Hes1* is also important for IL-17 production by γδ T cells in the periphery. Therefore, although Notch signaling is well known for its role in thymocyte development, it also regulates innate functions of γδ T cells in the thymus and in the periphery.

Submitted February 4, 2011; accepted May 8, 2011. Prepublished online as *Blood* First Edition paper, May 23, 2011; DOI 10.1182/blood-2011-02-334995.

The online version of this article contains a data supplement.

The publication costs of this article were defrayed in part by page charge payment. Therefore, and solely to indicate this fact, this article is hereby marked "advertisement" in accordance with 18 USC section 1734.

Methods

Mice

STAT3$^{flox/flox}$ mice,[18] *Tie-2-Cre* transgenic (Tg) mice,[19] and *RORc*$^{-/-}$ mice[20] were used. *Cβ*$^{-/-}$ mice were purchased from The Jackson Laboratory. *Hes1*$^{-/-}$ mice[21] and *Hes1*$^{flox/flox}$ mice[22] were kindly provided by R. Kageyama (Institute for Virus Research, Kyoto, Japan). IL-17–green fluorescent protein (GFP) reporter mice were kindly provided by Y. Iwakura (Institute of Medical Science, University of Tokyo, Japan). For analyzing disruption of floxed *STAT3*, genomic DNA from purified γδ T cells was analyzed by PCR.[23] For conditional ablation by inducing Cre recombinase driven by the IFN-inducible *MX-1* promoter, 5 × 300 μg of poly(I)-poly(C) (P-1530; Sigma-Aldrich) was injected intraperitoneally into 4-week-old mice at 2-day intervals. Fetal mice were obtained from timed matings in which the day of finding a vaginal plug was designated as day 0 of embryonic development. Mice were maintained in specific pathogen-free conditions at our institute. This study was approved by the Committee of Ethics on Animal Experiments in the Faculty of Medicine, Kyushu University. Experiments were carried out under the control of the Guidelines for Animal Experiments.

Cell preparations from various tissues

Single-cell suspensions were prepared from fetal thymi, adult thymi, adult spleens, lamina propria lymphocytes (LPLs), and intraepithelial lymphocytes (IELs), as described previously.[11]

Antibodies and flow cytometric analysis

FITC-conjugated anti-TCRγδ (GL3) and anti-CD4 (L3T4) mAb; PE-conjugated anti–mIL-17 (eBio17B7), anti-TCRγδ (GL3), anti-CD25 (PC61.5), anti-NK1.1 (PK136), and anti-cKit (2B8) mAb; allophycocyanin-conjugated anti-TCRγδ (GL3) and anti-B220 (RA3-6B2) mAb; and PerCP-eFluor710–conjugated anti-TCRγδ (GL3) mAb were purchased from eBioscience. FITC-conjugated anti-Vγ4 (UC3-10A6) and anti-Vγ5(536) mAbs, Alexa Fluor 647–conjugated anti–mIL-17 (TC11-18H10) mAb, and allophycocyanin-conjugated mIFN-γ (XMG1.2) mAb were purchased from BD Biosciences. PE-conjugated anti-CD27 (LG.3A10) mAb was purchased from BioLegend. PE-conjugated anti-Vγ5(536) mAb was purchased from Santa Cruz Biotechnology. Stained cells were analyzed on a FACSCalibur flow cytometer (BD Biosciences). Propidium iodide (1 μg/mL) was added to the cell suspension just before running on a flow cytometer to detect and exclude dead cells for the analysis of surface staining. The data were analyzed using CellQuest software Version 3.3 (BD Biosciences).

Intracellular cytokine staining

Cells were stimulated with 25 ng/mL of PMA (P-8139, Sigma-Aldrich) and 1 μg/mL of ionomycin (I-0634; Sigma-Aldrich) for 4 hours at 37°C; 10 μg/mL of brefeldin A (B-7651; Sigma-Aldrich) was added for the last 3 hours of incubation. After cells were stained with various mAbs for 20 minutes at 4°C, intracellular staining was performed according to the manufacturer's instructions (BD Biosciences).

qRT-PCR

Total RNA from hybridomas or cells sorted by FACSAria (BD Biosciences) was purified using the RNeasy Mini or Micro Kit (QIAGEN). The efficacy of cell sorting was consistently > 98%. The first-strand cDNA synthesis was done using Superscript I (Invitrogen) according to the manufacturer's instructions. Gene-specific primers were used as follows: *Hes1*, 5′-ACACCGGACAAACCAAAGAC-3′, 5′-ATGCCGGGAGCTATCTTTCT-3′; *Hes5*, 5′-CAAGGAGAAAAACCGACTGC-3′, 5′-GGCTTTGCTGTGTTTCAGGT-3′; *RORγt*, 5′-AGCTTTGTGCAGATCTAAGG-3′, 5′-TGTCCTCCTCAGTAGGGTAG-3′; *Notch1*, 5′-ACAACAACGAGTGTGAGTCC-3′, 5′-ACACGTGGCTCCTGTATATG-3′; *β-actin*, 5′-TGGAATCCTGTGGCATCCATGAAAC-3′, 5′-TAAAACGCAGCTCAGTAACAGTCCG-3′. Quantitative RT-PCR (qRT-PCR) was performed on an ABI PRISM thermal cycler (Applied Biosystems) using SYBR Premix Ex Taq (RP041A; Takara). The $2^{-\Delta\Delta Ct}$ equation was used to calculate the relative expression of target genes against that of *β-actin*.

Coculture with stromal cells

To induce T-cell differentiation in vitro, TSt-4 thymic stromal cells (TSt4/no) expressing murine Dll-4 gene (TSt-4/Dll4) were used as described previously.[24] Three thousand fetal thymocytes (E15) were cocultured on a layer of TSt-4/no or TSt-4/Dll4 cells in 24-well plates for the indicated days. Culture was performed without additional cytokines, and half of the medium was changed every 3 days.

Statistics

Statistical significance was calculated using the Student *t* test using Prism software Version 4.0a (GraphPad). $P < .05$ was considered to be statistically significant.

Results

STAT3 is dispensable for the development of IL-17–producing γδ T cells

STAT3 is an important transcription factor for the differentiation of Th17 cells, which are IL-17–producing CD4$^+$ αβ T cells.[25] To explore the roles of STAT3 in the development of IL-17–producing γδ T cells, we crossed *STAT3*$^{flox/flox}$ mice with *Tie2-Cre* Tg mice, because *STAT3*$^{-/-}$ mice are embryonically lethal.[26] Tie2 is a tyrosine kinase specifically expressed by hematopoietic progenitors and endothelial cells from E9.5.[27] We confirmed that the floxed *STAT3* allele was successfully disrupted in γδ T cells purified from the thymi and spleens of the conditional STAT3-deficient mice (Figure 1A). IL-17 production by γδ T cells in fetal and adult thymi was examined after brief stimulation with PMA and ionomycin, but there was no significant difference in the absolute number of IL-17–producing γδ T cells between STAT3-deficient and control mice (Figure 1B-C). Similarly, IL-17–producing γδ T cells were found equally in the periphery of the conditional STAT3-deficient and control mice (Figure 1D).

RORγt is partly required for the intrathymic development of IL-17–producing γδ T cells

RORγt is indispensable for the differentiation of IL-17–producing NKT cells and Th17 cells.[15,28] We next examined the role of RORγt in the development of IL-17–producing γδ T cells using RORγt-deficient (*RORc*$^{-/-}$) mice. As described previously,[20] the percentage of DP thymocytes was decreased in *RORc*$^{-/-}$ mice, although there was no significant decrease in the percentage or the absolute number of γδ T cells (supplemental Figure 1, available on the *Blood* Web site; see the Supplemental Materials link at the top of the online article). IL-17–producing γδ T cells in fetal and adult thymi were significantly decreased in *RORc*$^{-/-}$ and *RORc*$^{+/-}$ mice compared with *RORc*$^{+/+}$ mice (Figure 2A-B). However, there was no difference in the number of IL-17–producing γδ T cells between *RORc*$^{+/-}$ and *RORc*$^{-/-}$ mice. IL-17–positive cells in γδTCR-negative cells, which were detected in the adult thymi of *RORc*$^{+/+}$ or *RORc*$^{+/-}$ mice, were strikingly decreased in *RORc*$^{-/-}$ mice (Figure 2A). We found that most of these non-γδ T cells producing IL-17 expressed αβ TCR and CD4 (supplemental Figure 2). In contrast to the thymus, IL-17–producing γδ T cells were virtually